ANTIMICROBIAL PROPERTIES OF DOPED AND UNDOPED PLANT-BASED SYNTHESIZED ZINC OXIDE AND SILVER NANOPARTICLES

ABSTRACT

The process for the development of a reliable and ecofriendly metallic nanoparticle (NP) is an important step in biomedical application of nano technology. Zinc oxide nanoparticle (ZnONps) and silver nanoparticle (AgNps) is gaining attention in nanobiomedical due to their biocompatibility and antimicrobial activities. Therefore this study is aimed at evaluating the ecological synthesis of zinc oxide, silver doped silver and zinc oxide nanoparticle plus their antimicrobial properties. The green synthesis of ZnONps and AgNps was done using *Senna occiddentalis*. The green synthesized ZnONps and AgNps nanoparticles were characterized using UV-Visible spectroscopy, fourier transforms infra-red spectroscopy, Energy dispersive spectrum (EDS) and transmission microscope analysis (TEM). The NPs were tested for antimicrobial properties using agar well diffusion assays. The results indicated that the ZnONps and Ag NPs synthesized has particle size of 52.50 nm with intensity of 13.85 % at 393 nm wavelength, while AgNps were distributed at 83.40nm with intensity of 14 % at 331 nm wavelength and the particle size are 52.50 nm and 393 nm in wavelength, while silver nanoparticle were distributed around 83.40nm with intensity of 14 % and 331nm in wavelength. The surface morphology of the AgNps and ZnONps using TEM showed the presence of highly aggregation of spherical and irregular shape respectively. The EDS Spectrum of the AgNps showed optical absorption band peak at 3.0-3.5 KeV while ZnONps was at 1.0, 8.8, 9.8 KeV for mpH 7, 10, 11 and 12. The FT-IR spectral of bio-synthesized AgNp while ZnONps showed signal at 2893 and 3493 cm^{-1} corresponding to the –O-H stretch. The antimicrobial activity of AgNps produced dose dependent increase inhibition on *Streptococcus pyogenes, Escherichia coli, Staphylococcus auerus and Pseudomonas aeruginosa*, the activity of doped zinc and silver nanoparticles produced inhibition of S. pyogenes only amongst the tested organisms, however, ZnONps showed minimal antibacterial activities on *S.aureus* alone. However, it can be concluded that *Senna occidentalis* reduced Zinc acetate and Silver nitrate to Zinc oxide and silver ion respectively which provided minimum inhibitory effect on the selected microorganisms.

CHAPTER ONE

1.0 INTRODUCTION

1.1 Background to the Study

The ongoing research in the realm of nanoparticles, is due to the unique properties its offer. Atoms are the major building blocks in living tissue, and are measured using the nanoscale. Nano-sized particles allows interaction on molecules, this increases the efficacy and affinity when compared to biological molecules interacting with micro or macro sized particles (Li *et al.*, 2008). The high surface area to core ratio, is a unique physical characteristic in nanoparticles that is there are more atoms on the surface of the nanoparticle than deep within its core. This is particularly useful since surface atoms have free surfaces in comparison to core atoms, with the ability to create new and strong bonds, in essence, nanoparticles are more reactive in comparison to micro and macro particle which have more core than surface atoms (Binns, 2010). In comparison to the same material in bulk, nano particles can be arranged easily in a number configurations due to their high surface to core ratio, making them easily manipulated and used in various applications. The greater l vibrations expressed by surface atoms in comparison to core atoms in any given material regardless of particle size, contribute to the lower melting temperature in nanomaterials compared to the same material inbulk (Buffat and Borel, 1976). This might be of advantage when using nanomaterials to construct porcelain fused to metal (PFM) crowns, cast post and cores, or denture frameworks.

Nanoparticles are very small sized particles with high catalytic reactivity, thermal conductivity, non-linear optical performance and chemical steadiness owing to its large surface area to volume ratio. Agarwal *et al.* (2017). Nanoparticles have s being considered as nano antibiotics because of their efficacy in antimicrobial activities. Nanoparticles have been integrated into various industrial uses, like health, food, feed,

space, chemical, and cosmetics industry of consumers this calls for a green and ecos-friendly approach to their synthesis Agarwal *et al.* (2017).

Two approaches have been suggested for nanoparticle synthesis: Bottom up and top down approach. The top–down approach involves millings of large macroscopic particle. It involves synthesizing large-scale patterns initially and then reducing it to nanoscale level through plastic deformation Agarwal *et al.* (2017). This approach cannot be employed for large scale production of nanoparticles because it is costly and slow. Inter ferometric Litho- graphic (IL) is the most common technique which employs the role of top–down approach for nanomaterials synthesis. This technique involves the synthesis of nanoparticles from already miniaturized atomic materials through self-assembly. Agarwal *et al.* (2017). This includes formation through physical and chemical means. It is a less expensive approach. It is based on kinetic and thermodynamic equilibrium approach. The kinetic approach involves MBE (Molecular Beam Epitaxy) Agarwal *et al.* (2017). Agarwal *et al.* (2017) study reveals that various inorganic metal oxides can be manufactured, such as tin oxide (TiO_2), copper oxide (CuO), and zinc oxide (ZnO), among these three ZnO is more economical. US Food and Drug Administration (US FDA) identified ZnO as one of the good semiconductors because of its good band gap it can be used as cosmetic sunscreen lotions, anticancer, anti-diabetic, antibacterial, antifungal because of its UV filtering features. More so, ZnO is used to remove sulphur and arsenic from water, it also has protein adsorption properties, and can also be applied in dental surgery. ZnONps have piezoelectric and pyroelectric properties. They are used for disposal of aquatic weed which is resistant to all type of eradication techniques like physical, chemical and mechanical means.

ZnONPs have been reported in different morphologies like nano-flake, nanoflower,nano-belt, nano-rod and nano-wire. However, Silver nanoparticles (AgNPs)

are increasingly used in various fields, including medical, food, health care, consumer, and industrial purposes, due to their unique physical and chemical properties. These include optical, electrical, and thermal, high electrical conductivity, and biological characteristics (Konrad *et al.,* 2013). Due to their unique properties, they have been used for several applications, including as antibacterial agents, in industrial, household, and healthcare-related products, in consumer which includes food products and also, they are also used as medical device coatings, optical sensors, and in cosmetics, in the pharmaceutical industry, in diagnostics, orthopedics, drug delivery, as anticancer agents, and have also help to improve the tumor-killing effects of anticancer drugs (Konrad *et al.,* 2013).

1.2 Statement of the Research Problem

The emergence of bacterial resistance and multiresistance to antibiotics represent a major public health concern in Nigeria and in the entire world. Globally, antibiotic drug resistance causes an estimated 1 million death each year, if this continues, it is projected that by 2050-2060 antimicrobial resistance could result in over 10million deaths per year and over 200trillion USD will be lost globally. (WHO 2012, ACDC 2018). Antimicrobial materials used in the clinical setting today are beset by significant short falls including weak antimicrobial activities, difficulty in monitoring and extending the antimicrobial functions as well as difficulty in functioning in a dynamic environment (Martinez *et al.,* 2010). Thus, effective and long term antibacterial and bio-film preventing materials constitute an immediate need in medicine.

Metals and non-metals oxides have been widely studied for their antimicrobial activities. However, most of the currently available methods or techniques for synthesizing these nanoparticles are expensive, environmentally harmful and inefficient

with respect to material and energy use, this calls for a better and eco-friendly method for synthesizing nanoparticles.

1.3 Justification for the Research Problem

Senna occidentalis have been widely used for centuries by African, American and Indian tribes principally as a antimalarial or antimicrobial medicine, as a laxative or hepatoprotective (Lombardo *et al.*, 2009). Scientific data have revealed that *Senna occidentalis* comprise a rich source of phenolic derivatives with important biological and pharmacological properties (Ogunkunle *et al.*, 2006). *Senna occidentalis* are readily available in sahara region and the sub-sahara regions.

Metals and non-metals oxides are well known for their highly potent antibacterial effects. These include Silver (Ag), Zinc oxide (ZnO), Iron oxide (Fe_3O_4). Most metal oxide nanoparticles exhibit bacterial properties through reactive oxygen species (ROS) generation, although some are effective due to their physical structure and metal ion release.

Silver (Ag) and ZnO oxide finds a very promoient place in the field of doped nanoparticles in biomedical field. Silver (Ag) is a transition metal, which has properties like the electricial conductivity and reflectively of any metal. Kluel *et al.*, 2000.

Zinc oxide (ZnO) is widely renowned for its antibacterial uses. The main reasons for this is the free electrons and positive holes which are generated when Zinc oxide, having a high band is bombarded with an energy equal or higher than this band gap energy. But this free energy electrons and holes recombined quite fast, not allowing them enough time to take part in any chemical reactions. So, the electrons and the holes should be captured by any material which exist on the surface (ions, molecules etc) or by some surface traps (Morales Flores *et al.*, 2011). The doping comes as a solution to this problem and thus several researches have been done to enhance its activity by

doping it with silver. Silver (Ag) and Zinc oxide precussors such as Silver nitrate (v) and Zinc acetate dehydrate are readily available and cheap.

In synthesizing this nanoparticles, the biosynthesis approach has been proposed as an alternative to reduce the usage of hazardous chemical compounds and harsh reaction conditions in the production of these nanoparticles.

Therefore, this research work focuses on using aqueous leaf extract of Senna occidentalis to synthesize Ag, ZnO nanoparticles and doped Silver and Zinc oxide nanoparticles and to evaluate their antimicrobial properties.

1.4 Aim and Objectives of the Study

The aim of this study is to evaluate plant-based-synthesis of Zinc oxide, silver nanoparticle and doped silver and zinc oxide nanoparticles along with their anti-microbial activities.

Specific Objectives are to;

i. Determine the qualitative phytochemical constituents of *Senna Occidentalis* using aqueous leaf extract.
ii. Synthesize Zinc oxide (ZnO) and Silver (Ag) nanoparticles using aqueous leaf extract of *Senna occidentalis* by varying pH condition
iii. Characterize the zinc oxide (ZnO) and silver (Ag) nanoparticles using UV visible spectroscope, Zeta sizer, transmission electron microscopy and frontier transformed infrared spectroscopy
iv. Evaluate the antimicrobial properties of silver, zinc and doped zinc/silver nanoparticles using microorganisms: *Gram positive bacteria: S. pyrogenes, S. aureus* gram negative bacteria: S. *aeruginosa and E. coli*

CHAPTER TWO

2.0 LITERATURE REVIEW

2.1 Nanotechnology

Nanotechnology is the art and science of material engineering in a scale of less than 100 nm (Anisa *et al.,* 2003). It revolutionizes the medical and dental fields by enhancing mechanical and physical characteristics of materials, this has helped introduced new diagnostic techniques and nano-delivery scheme (Kanaparthy and Kanaparthy, 2011). Inan effort to create an eco-friendly socially acceptable nanotechnology, the United States National Human Genome Research Institute proposed a new techniques to the development process of new technology. This was accomplished by addressing the ethical, legal, and social incriminations before Nano-products reach the market to easily modify and regulate during the early stages of production (Ramsay, 2001; Macnaghten *et al.,* 2005).

The current research in the field of nano, is due to the peculiar characteristics nanoparticles offer. Atoms are the building blocks in living tissue, and these atoms are measured using the nanoscale. Instituting nano-sized particles allows for a contact on a molecular level, by that increasing the overall effectiveness and empathy in comparison to biological molecules interacting with micro or macro sized particles (Li *et al.*,2008).

2.2 Nanoparticles

Nanoparticles are defines as particles liquid or solid particles with a size range of 1-100 nm**.** NPs are not simple molecules and therefore composed of three layers i.e. (a) The surface layer which may be operationalized with diverse small molecules, metal ions, surfactants and polymers. The shell layer, which is chemically different material from the core in all facets, and (c) The core, which is originally the central portion of the NP and usually refers to as the NP itself (Shin *et al*., 2016). Owing to such unique

characteristics, these materials got huge interest of researchers indifferent disciplinary fields.

The NPs can be applied for drug delivery, chemical and biological sensing, gas sensing, CO_2 capturing and other related applications (Shaalan *et al*., 2016).

2.2.1 Classification of nanoparticles

NPs are broadly divided into various categories depending on their morphology, size and chemical properties. Based on physical and chemical characteristics, some of the well-known classes of NPs are given as below.

2.2.1.1 Carbon-based nanoparticles

Fullerenes and carbon nanotubes (CNTs) constitutes two major classification based NPs. Fullerenes are carbon-based NPs that contain nano material that are made of spherical hollow cage such as allotropic forms of carbon. They have created notable commercial interest in nano composites for commercial applications such as fillers, good gas adsorbents for environment redress and as support medium for different organic and organic catalysts. (Mabena *et al*., 2011).

2.2.1.2 Metal nanoparticles

Metal NPs are entirely made of the meal precursors. Due to well-known localized surface plasm on resonance (LSPR) characteristic, these NPs posses' peculiar electrical properties. NPs of the alkali and nonmetals i.e. Cu, Ag and Au have widely absorption band in the evident zone of the electromagnetic solar spectrum. The facet, size and shape controlled synthesis of metal NPs significant in present day edge material (Dreaden *et al*., 2012). Due to their advanced optical properties, metal NPs are employed in many researches. Gold NPs coating is widely used for the smapling of SEM, to improve the electrical stream, which helps in obtaining high and good quality SEM images.

2.2.1.3 Silver and zinc oxide nanoparticles

Metallic oxide nanoparticles have been known for their fascinating utilization in various spheres of electronics, energy store house devices, ecological remediation, microbe blockage, medical implants and optical appliances. Thus, the synthesis and engineering of metal oxide nanoparticles finds great scope in the modern generation of urbanization and industrialization (Murphy *et al.,* 2005). For environmental redress in a continuous way, metal oxides are of prime importance. Water purification has been examined with different types of metal oxides and results were suggestive of that all metallic oxide nanoparticles.

2.2.1.4 Zinc nanoparticles

Zinc oxide (ZnO) has large potential for photocatalysis and the significance of its steady nature in disclosure to light is due to wider band gap of 3.37 eV, improved activity and lower cost. ZnO has been applied on industrial scale for architectural conformation and semiconducting characteristics (Mishra *et al.,* 2012). ZnO is found to surpass TiO_2 in water redress due to generation of radical oxygen species (ROS) consecutively executing remarkable solidified outputs, as well as increasing reaction sites due to higher surface reactivity (Chang *et al.,* 2013).

2.2.1.5 Silver nanoparticles

Ag is considered as one of the best options in selection of dopant for its potential in generation of electrical field and subsequent improvement in galvanic attributes due to surface plasmon resonance (SPR) (Wu *et al.,* 2006).

2.3.1.6 Doped Zinc oxide and silver nanoparticles

ZnO doped Ag nanoparticles have unique properties, doping of Ag into ZnO is expected to modify the absorption, physical and chemical properties of ZnO. To ehance the

antibacterial activity of ZnO, different physiochemical properties such as particle size, crystallinity index and optical properties should be modified by doping with metal or non-metal (Wang *et al.,* 2004).

2.2.3 Ceramics nanoparticles

Ceramics NPs are inorganic nonmetallic solids, synthesized using heat and cooling. They can be found in amorphous, polycrystalline and hollow forms (Sigmund *et al*., 2006). Therefore, the NPs are getting great interest of researchers due to their applications degradations of dyes, and imaging applications (Thomas *et al*., 2015).

2.2.4 Semiconductors nanoparticles

Semiconductor materials maintain properties between metals and nonmetal so are found various uses in literature due to these properties (Ali *et al*., 2017). Semiconductor Nps possess a wide and gap band gaps and therefore showed advantageous alteration in their properties with band gaps adjustment (Sun, 2000). Therefore, they are very significant materials in photo catalysis, photo optics and electronics devices. As an example, different semiconductor Nps have found exceptionally good use in waters splitting applications, due to their acceptable band gap and edge positions (Hisatomi *et al*., 2014).

2.2.5 Polymeric nanoparticles

These are normally organic based NPs collectively known as polymer nanoparticle (PNP). They are more of nanosphere somano capsular forms (Mansha *et al.*, 2017). The nanosphere are matrix particles whose overall mass is generally solid and the other molecules are absorbed at the outer boundary of the spherical surface while the nanocapsular the solid mass is encapsulated within the particle completely (Rao and Geckeler, 2011). The NPs are readily functionalized and thus possess bundles of applications in the literature (Abdellah and Abouelmagd, 2016).

2.3 Applications of Nanoparticles

Nano crystalline material provides everything interesting substance for material science since their properties deviate from respective bulk material in a size dependent manner. Manufacture NPs display physiochemical characteristics that induce unique electric, mechanical, optical and imaging properties that are extremely looked-for in certain applications within the medical, commercial, and ecological sectors (Dong *et al*., 2014). NPs focuses on the characterization, designing and engineering of biologicals as well as non-biological structure less than 100 nm, which show unique and novel functional properties. The potential benefits of nanotechnology have been documented by many manufactuer at high, low level and marketable products which are already being mass produced such as micro electronics, aero-space and pharmaceutical industries (Weiss *et al*., 2006). Among the nano technology consumers products to date, health fitness products from the largest category, followed by electronic and computer category as well as home and garden category. Nano technology has been touted as the best revolution in many industries including food processing and packaging.

2.3.1 Diagnostic biosensor

In a strive to improve upon medical diagnostics, the idea of nano-biosensing was introduced. A biosensor is ‘‘analytical device which include a biologically energetic element with a suitable physical transformer to create a measurable mixture corresponding to the concentration of chemical species in any type of sample” (Touhami, 2014). Biosensors were induced in 1962 by Clark and Lyons (1962), followed by current broad research and evolution of this promising technology by employing diverse observation principles, leading to possible applications in public health, environmental monitoring, and food safety (Touhami, 2014). In an effort to improve the biological recollection process and overall bioreceptor execution,

nanobioreceptors were introduced, including nanotubes, nanowires, and nano-dots in the sensing string (Sagadevan and Periasamy, 2014).

Nanobiosensors are also amenable, as they are easily replaced and damaged in response to very low forces, therefore, tactful enough to detect breaking of chemical bonds (Arlett *et al.,* 2011). This is ascribed to its nano size effects, as the high surface area to core ratio increases the level of tactfulness, electrical properties, and response time of the biosensor (Sagadevan and Periasamy, 2014).

Metallic nanoparticles such as gold, silver, platinum, and palladium are commonly included in nanobiosensor transformation/bioreception systems as they are able to swiftly react with most biological molecules without affecting their activity (Sagadevan and Periasamy, 2014). Gold nanoparticles have been widely studied, divulging an ability to improve the electronic signal when the bioreceptor detects the analyte at very minimal concentrations, for example, gold nanoparticle mutated DNA bioreceptor detects an analyte at a concentration as minimal as 0.05 nm (Su *et al.,* 2003) Also, carbon nanotubes were utilized for the detection of circulating cancer cells in the body. The carbon nanotubes were arranged by the layer-by-layer assembly technique and then linked chemically to antibodies of specific carcinogenic marker which specifically binds to cancer cells, thus, providing an effective and useful diagnostic tool (Hasanzadeh and Shadjou, 2016). This not only enhances the performance of biosensors, it also creates an opportunity to manufacture very small sizes of Nano-biosensors that can be worn or even implanted as opposed to larger sizes of conventional biosensors that are not feasible and cost more to manufacture (Touhami, 2014).

2.3.2 Preventive dentistry

Researchers have developed a nano-toothbrush, by including nanogold or nanosilver colloidal particles between toothbrush prickle (Raval *et al.,* 2016). In addition to its ability to enhance upon automate plaque removal, researchers reported antibacterial effect of the added gold or silver which could ultimately lead to a great reduction in periodontal disease.

Oral hygiene products such as toothpastes and mouth wash solutions are also nano-modified according to recent reports. Nano-calcium fluoride, added to mouth wash products have been reported to reduce reduce dentine permeability, and increase labile fluoride concentration in oral fluid (Sun and Chow, 2008). Toothpastes containing calcium carbonate nanoparticles and 3 % nanosized sodium trimetaphosphate have been reported to promote demineralization of early carious lesions in comparison to a conventional toothpaste with no nano-additives (Danelon *et al.,* 2015). Ebadifar *et al.* (2017), reported that toothpastes containing nano-hydroxyapatite crystals (nHA) significantly increased micro hardness values in human enamel following an erosive challenge, in comparison to the same toothpaste without nHA. However, the benefits of a nHA containing toothpaste was first reported in Japan in the 1980s (Kani *et al*., 1989). In 1983, three primary schools were enrolled in their 3-year clinical study. The schools were provided with toothbrushes and toothpastes. One school was given a 5 % nHA based tooth paste, while the other two schools were provided with controls. Students were instructed to brush using the provided toothbrush and toothpaste every day during school hours and under a teacher's supervision. Results gathered revealed a 56 % reduction in caries incidence in school children brushing with a nHA toothpaste in comparison to the control groups (Kani *et al.,* 1989). However, the higher reparative capacity of nanomaterials in comparison to the same material in a micro or macro scale, was attributed to the fact that the inorganic building blocks in enamel are 20–40 nm in

size, making it logical to assume a higher affinity to nanosized particles (Robinson *et al.,* 2004; Tao *et al.,* 2007).

2.3.3 Drug delivery

Benefits of using ZnONps for the drug delivery were derived from their two main basic properties. First of all, due to their smaller size, nanoparticles can penetrate through smaller capillaries and are absorbed by the cells, allowing an efficient accumulation of drugs at the target sites. Second, the use of biodegradable materials for the preparation of nanoparticles allows the prolonged discharge of drugs within the site targeted over a period of days or even weeks (Shamsuzzaman *et al.* 2015) Role of synthesized ZnO NPs in drug release by using the drug metronidazole benzoate was studied (Ghasemi, 2016) by observing its diffusion through egg membrane. It revealed that the presence of ZnO NPs with the drug has much effect on the biological membrane.

2.3.4 Application in the environment

The increasing area of engineered NPs in industrial and household application leads to the release of such materials into the environment. Assessing the risk of these NPs in the environment requires sound understanding of their mobility, reactivity, ecotoxicity and persistency (Ripp *et al*., 2011). The engineering material application can increase the concentration of NPs in ground water and soil which presents the most significant exposure avenues for assessing environmental risks (Masciangioli and Zhang, 2003). Due to high surface to mass ratio, natural NPs plays an important role in the solid/water partitioning of contaminates absorbed to the surface of NPs, co-precipitated during the formation of natural NPs or trapped by aggregation of NPs. The interaction of contaminants with NPs is dependent on the NPs characteristics, such as size, composition, morphology, porosity, aggregation/disaggregation and aggregate structure. The luminophores are not safe

in the environment and are protected from the environmental oxygen when they are doped inside the silican network (Swadeshmukul *et al*., 2001).

2.3.5 Application in electronics

There has been growing interest in the development of printed electronicx in last few years because printed electronics offer an attraction to traditional silicon techniques and the potentials for low cost, large area electronics for flexible displays, and sensors. Printed electronics with various functional inks containing NPs such as metallic NPs, organic electronic molecules, CNTs and ceramics NPs have been expected to flow rapidily as as mass production process for new type of electronic equipment. Unique structural, optical and electrical properties of one dimensional semi conductors and metals are the key structural block for a new generation of electronic, sensors and photomaterial (Holzinger *et al*., 2014). The good example of the synergism between secientific discovery and technological development is the electronic industry, where discoveries of new semiconducting material result in the revolution from vaccumed tubes to diodes and transistors, and eventually to moniaturechips

2.4 Application of silver nanoparticles

Nano sized metallic particles are unique and can considerably change physical, chemical, and biological properties due to their surface-to-volume ratio; therefore, these nanoparticles have been exploited for various purposes (Bu *et al.,* 2012).

Silver nanoparticles (AgNps) are increasingly used in many fields, such as industry, household, and healthcare as (Konrad *et al.*, 2013). AgNps have been frequently used in many textiles, keyboards, wound dressings, and biomedical devices (Thanha *et al.,* 2010).

In order to fulfill the requirement of AgNPs, various methods have been adopted for synthesis. Generally, conventional physical and chemical methods seem to be very

expensive and hazardous (Franci, 2015). Interestingly, biologically-prepared AgNPs show high yield, solubility, and high stability. Among several synthetic methods for AgNPs, biological methods seem to be simple, rapid, non-toxic, dependable, and green approaches that can produce well-defined size and morphology under optimized conditions for translational research. In the end, a green chemistry approach for the synthesis of AgNPs shows much promise. After synthesis, precise particle characterization is necessary

2.5 Features of Zinc Oxide Nanoparticles

2.5.1 Bio-imaging of Zinc oxide nanoparticles

In preclinical research, fluorescence imaging is extensively utilized as it is convenient and inexpensive (Fowsiya *et al.,* 2016). As ZnO nanomaterials have essential excitonic blue and near-UV emission, which has green luminescence associated with vacancies (Debrucdkar, 2016) and for cellular imaging, there are numerous reports existing inprevious studies on the utilization of ZnO nanomaterials. For cancer cell imaging, transferrin-conjugated green fluorescent ZnONps were utilized with least cytotoxicity (Mhisra, 2015). According to some research, ZnONps were adulterated with various cations such as Co, Cu, or Ni, and in aqueous colloidal solutions, and stabilized, which was employed in different cells for cellular imaging studies (Shamsuzzaman *et al.*, 2015).

2.5.2 Biosensors based on Zinc oxide nanoparticles

Biosensors are extensively utilized in food industry, environmental monitoring, and healthcare and in chemical or biological analysis. Examples for biosensors are electrochemical, photometric, piezoelectric, and calorimetric among others when categorized based on the detection principless. Nanomaterials, either as uncombined or as combination with biologically active substances, are attaining ever increasing

awareness because of their capability to deliver a suitable platform for developing high-performance biosensors, which is due to their distinctive features (Amin *et al.,* 2012). For instance, the higher surface area of nanomaterials could be utilized for immobilizing numerous biomolecules such as antibodies, enzymes, and other proteins. Moreover, they could be permitted for a direct electron transfer among the electrodes and the active sites of the biomolecules. ZnO nanomaterials also provide numerous desirable traits apart from semiconducting properties such as biosensing, strong adsorption capability, high isoelectric point, and high catalytic efficiency which are appropriate for adsorption of certain proteins such as antibodies and enzymes with less IEPs (isoelectric points) by electrostatic interaction (Yedurkar *et al.,* 2015). Moreover, the favorable conditions of nanomaterials to be used in biosensors are lower toxicity, higher electron transfer capability, higher surface area, and better biocompatibility or stability (Henley *et al.,* 2008). Nanoparticles significantly improved hardness levels, flexural strength, and fracture toughness of the heat cured PMM Adenture base. Nano sized fillers were used due to their superior dispersion properties, less aggregation potential, and biocompatibility with the organic polymer. Nano zirconium not only improved physical properties of denture bases during the construction phase, they were reported to improve the transverse strength of a repaired denture base as well (Gad *et al.,* 2016).

The addition of nanoparticles did not affect the hydrophility and water uptake of denture silicons following immersion in artificial saliva for 16 weeks. However, the nano-modified chlorhexidine coatings released soluble chlorhexidine into artificial saliva, with a slow and sustained release by the chlorhexidine-HMP coating, and a rapid, more concentrated release by the chlorhexidine-TP and chlorhexidine-TMP coatings. The chlorhexidine-HMP coating proved to be the most effective in its antifungal activity by inhibiting the metabolic activity of *Candida albicans*. These coatings might potentially

become clinically essential for insuring longevity of the dental prosthesis and maintenance of oral health at a much lower cost. Nano-particle impregnated luting cements proved to be significantly effective in increasing the bond strength to enamel and dentine in comparison to conventional luting cements. They bond particularly well to dentin, as these very small sized particles penetrate deeper into the dentinal tubules, therefore, increasing the elastic modulus, and reducing polymerization shrinkage (Sadat-Shojai *et al.,* 2010).

2.6 Synthesis of Silver Nanoparticles

Generally, the synthesis of nanoparticles has been carried out using three different approaches, including physical, chemical, and biological methods.

In physical methods, nanoparticles are prepared by evaporation-condensation using a tube furnace at atmospheric pressure (Lee *et al.,* 2005). Conventional physical methods including spark discharging and pyrolysis were used for the synthesis of AgNPs (Magnusson *et al.,* 1999). The advantages of physical methods are speed, radiation used as reducing agents, and no hazardous chemicals involved, but the downsides are low yield and high energy consumption, solvent contamination, and lack of uniform distribution (Mafune *et al.,* 2000).

2.6.1 Chemical methods

These methods use water or organic solvents to prepare the silver nanoparticles (Vilchis-Nestor *et al.,* 2008). This process usually employs three main components, such as metal precursors, reducing agents, and stabilizing/capping agents. Basically, the reduction of silver salts involves two stages (1) nucleation; and (2) subsequent growth. In general, silver nanomaterial can be obtained by two methods, classified as “top-down” and “bottom-up” (Chen *et al.,* 2012). The “top-down” method is the mechanical grinding of bulk metals with subsequent stabilization using colloidal protecting agents

(Dan *et al.,* 2012). The "bottom-up" methods include chemical reduction, electrochemical methods, and sono-decomposition. The major advantage of chemical methods is high yield, contrary to physical methods, which have low yield. The above-mentioned methods are extremely expensive. Additionally, the materials used for AgNps synthesis, such as citrate, borohydride, thio-glycerol, and 2-mercaptoethanol are toxic and hazardous (Patil *et al.,* 2016). Apart from these disadvantages, the manufactured particles are not of expected purity, as their surfaces were found to be sedimented with chemicals. It is also very difficult to prepare AgNps with a well-defined size, requiring a further step for the prevention of particle aggregation (Tran *et al.,* 2013). In addition, during the synthesis process, too many toxic and hazardous byproducts are excised out. Chemical methods make use of techniques such as cryochemical synthesis , laser ablation (Luo *et al.,* 2005), lithography (Hsu *et al.,* 2012), electrochemical reduction (Chen *et al.,* 2007), laser irradiation (Natsuki *et al.,* 2007), sono-decomposition (Natsuki *et al.,* 2013), thermal decomposition (Natsuki *et al.,* 2015), and chemical reduction (Cho *et al.,* 2004). The advantage of the chemical synthesis of nanoparticles are the ease of production, low cost, and high yield; however, the use of chemical reducing agents are harmful to living organisms. Recently, Abbasi *et al.* explained a detailed account of synthesis methods, properties, and bio-application of AgNPs.

2.6.2 Green chemistry approach for the synthesis of Silver Nanoparticles

To overcome the shortcomings of chemical methods, biological methods have emerged as a viable options. Biologically-mediated synthesis of nanoparticles have been shown to be simple, cost effective, dependable, and environmentally friendly approaches and much attention has been given to the high yield production of AgNPs of defined size using various biological systems including bacteria, fungi, plant extracts, and small

biomolecules like vitamins and amino acids as an alternative method to chemical methods—not only for AgNps, but also for the synthesis of several other nanoparticles, such as gold and graphene (Cho *et al.,* 2005). Bio-sorption of metals by gram-negative and gram-positive bacteria provided an indication for the synthesis of nanoparticles before the flourishing of this biological method; however, the synthesized nanomaterials were aggregates (Duran *et al.,* 2007). In green chemistry approach, several bacteria, including *Pseudomonas stutzeri*, *Lactobacillus* strains, Bacillus Licheniform is, *Escherichia coli* (E. *coli*), *Brevibacterium*. Fungi including *Fusarium oxysporum*, *ganoderma neo-japonicums* have been used. Also, plant extracts such as *allophylus* cobbe, *Artemisia princeps*, *Typha angustifolia* have been utilized. In addition to these, several biomolecules, such as biopolymers, starch, *fibrinolytic* enzymes, and amino acids, were being reported. The biological synthesis of nanoparticles depends on three factors, including (a) the solvent; (b) the reducing agent; and (c) the non-toxic material. The major advantage of biological methods is the availability of secondary metabolites in the synthesis process, elimination of the extra step required for the prevention of particle aggregation, and the use of biological molecules for the synthesis of eco-friendly and pollution-free AgNps. Biological methods seem to provide controlled particle size and shape, which is an important factor for various biomedical applications. Using bacterial protein or plant extracts as reducing agents, have been reported to control the shape, size, and monodispersity of the nanoparticles (Tanha *et al.*, 2012). The other advantages of biological methods are the availability of a vast array of biological resources, a decreased time requirement, high density, stability, and the ready solubility of prepared nanoparticles in water. The biological activity of AgNPs depends on the morphology and structure of AgNPs, controlledby size and shape of the particles.

As far as size and shape are concerned, smaller size and truncated-triangular nanoparticles seem to be more effective and have superior properties.

2.7 Synthesis of Zinc Oxide Nanoparticles (ZnONps)

Zinc oxide (ZnO) is generally recognized as safe (GRAS) compound (U.S. FDA: 21CFR182.8991) and exhibits minimal toxicity to humans. Zinc oxide nanoparticles have high photo catalytic activity and are more biocompatible than TiO_2 (Sirelkhatim *et al.,* 2015). Zinc oxide is used widely in the food industry to preserve colours and prevent spoilage due to its antimicrobial activity. Zinc oxide nanoparticles have pronounced antimicrobial activity due to their high surface to volume ratio and surface abrasiveness of the nanostructures. ZnONps can inhibit the growth of both gram positive and gram negative bacteria. Gram positive bacteria including *S. aureus*, *Streptococcus pyogenes* and *Enterococcus faecalis* have shown 95 % growth inhibition in the presence of ZnO (Sirelkhatim *et al.,* 2015). ZnONps have potent antimicrobial activity against common food pathogens such as *Campylobacter jejuni*, *E.coli*, *Salmonella spp.*, *Listeria monocytogenes,* and *S. aureus* indicating its usefulness as a food preservative (Seil and Webster, 2012). Applications of ZnO include antibacterial creams, lotions, ointments and deodorants. Further, self-cleaning glass and ceramics consisting of ZnONps is another novel application (Fateh *et al.,* 2014). The antimicrobial properties of ZnONps are attributed to the intracellular accumulation of ZnONPs which result in damage to the cell wall and disruption of DNA replication. Inside the cells, the NPs release metal ions, generate reactive oxygen species (ROS) and accumulate in the bacterial membrane. Studies have shown the strong ROS generating potential of ZnONps, suggesting it has an important role in bacterial killing, including cell wall damage, increasing membrane permeability, internalization of NPs due to loss of proton motive force and uptake of toxic dissolved zinc ions (Sirelkhatim *et al.*, 2015).

2.8 Analytical Techniques for Characterization of Nanoparticles

The following are the analytical techniques used for the characterization of nanoparticles:

2.8 .1 Ultra Violet-Visible spectroscopy

UV-visible spectroscopy is a very useful and reliable technique for the mary characterization of synthesized nanoparticles that is used to monitor the synthesis and stability of AgNPs (Luo *et al.,* 2015). AgNPs have unique optical properties which make them strongly interact with specific wavelengths of light (Rivero *et al.,* 2013). In addition, UV-visible spectroscopy is fast, easy, simple, sensitive, and selective for different types of NPs, It requires only a short period time for measurement, and calibration of suspensions . The AgNPs, conduction and valence band lie very close that makes electrons move freely. These free electrons give rise to a surface plasmon resonance (SPR) absorption band, occurring due to the collective oscillation of electrons of silver nanoparticles in resonance with the light wave (Tanha *et al.,* 2013). The absorption of AgNPs depends on the particle size, dielectric medium, and chemical surroundingss. Observation of this peak—assigned to a surface plasmon—is well documented for various metal nanoparticles with sizes ranging from 2 to 100 nm (Tsunga *et al.,* 2008). The stability of AgNPs prepared from biological methods was observed for more than 12 months, and an SPR peak at the same wavelength using UV-visible spectroscopy was observed.

2.8.2 X-ray diffraction (XRD)

X- ray diffraction is a popular analytical technique which has been used for the analysis of both molecular and crystal structures (Sondi *et al.,* 2004), qualitative identification of various compounds. This have because for quantitative resolution of chemical species (El-Nour *et al.,* 2010), measuring of the degree of crystallinity (Smeta *et al.,* 2005) and

isomorphous substitutions, particle sizes. When X-ray light reflects on any crystal, it leads to the formation of many diffraction patterns, and the patterns reflect the physic chemical characteristics of the crystal structures. In a powder specimen, diffracted beams typically come from the sample and reflect its structural physico-chemical features. Thus, XRD can analyze the structural features of a wide range of materials, such as inorganic catalysts, superconductors, biomolecules, glasses, polymers, and so on (Wakud *et al.,* 2008). Analysis of these materials largely depends on the formation of diffraction patterns. Each material has a unique diffraction beam which can define and identify by comparing the diffracted beams with the reference database in the Joint Committee on Powder Diffraction Standards (JCPDS) library. The diffracted patterns also explain whether the sample materials are pure or contain impurities. XRD is a primary technique for the identification of the crystalline nature at the atomic scale (Ana *et al.,* 2009). This techniques has been used to measure phase identification, conduct quantitative analysis, and to determine structure imperfections in samples from various disciplines, such as geological, polymer, environmental, pharmaceutical, and forensic sciences. The applications have recently extended to the characterization of various nano-materials and their properties.. The working principle of X-ray diffraction is Bragg's law *et al.,* 2014). Typically, XRD is based on the wide-angle elastic scattering of X-rays . Although XRD has several merits, it has limited disadvantages, including difficulty in growing the crystals and the ability to get results pertaining only to single conformation/binding state (Iravani *et al.,* 2014). Another drawback of XRD is the low intensity of diffracted X-rays compared to electron diffractions (Kholoud *et al.,* 2010).

2.8.3 Dynamic light scattering (DLS)

Physicochemical characterization of prepared nanomaterials is an important factor for the analysis of biological activities using radiation scattering techniques (Iravani *et al.,*

2014). DLS can probe the size distribution of small particles, scale ranging from submicron down to one nanometer in solution or suspension (Lenon *et al.,* 2007). Dynamic light scattering is a method that depends on the interaction of light with particles. This method can be used for the measurement of narrow particle size distributions, especially in the range of 2–500 nm (Tsuruga *et al.,* 2008). Among the techniques for the characterization of nanoparticles, DLS is the most commonly used is (Iravani *et al.,* 2014). DLS measures the light scattered from a laser that passes through a colloid, and mostly relies on Rayleigh scattering from the suspended nanoparticles (Iravani *et al.,* 2014). The modulation of the scattered light intensity as a function of time is analyzed, and the hydrodynamic size of particles can be determined (Lee, 2015). To evaluate the toxic potential of any nanomaterial, its characterization in solution is essential (Gates *et al.,* 1995). Therefore; DLS is mainly used to determine particle size and size distributions in aqueous or physiological solutions (Iravani *et al.,* 2014). The size obtained from DLS is usually larger than TEM (Transmission electron microscopy), which may be due to the influence of Brownian motion.

DLS is a nondestructive method used to obtain the average diameter of nanoparticles dispersed in liquids. It has the special advantage of probing a large quantity of particles simultaneously.

2.8.4 Fourier transform infrared (FTIR) spectroscopy

Fourier Transform Infrared is able to provide accuracy, reproducibility, and favorable signal-to-noise ratio. By using FTIR spectroscopy, it becomes possible to detect small absorbance changes on the order of 10^{-3}, which helps to perform different spectroscopy. Where one could distinguish the small absorption bands of functionally active residues can be distinguish from the large background absorption of the entire protein. FTIR spectroscopy is frequently used to find out whether biomolecules are involved in the

synthesis of nanoparticles, which is more pronounced in academic and industrial research (Iravani *et al.*, 2014). Furthermore, FTIR has also been extended to the study of nano-scaled materials, such as confirmation of functional molecules covalently grafted onto silver, carbon nanotubes, graphene and gold nanoparticles, or interactions occurring between enzyme and substrate during the catalytic process (Magnusson *et al.*, 1999). Furthermore, it is a non-invasive technique which makes FTIR spectrometers over dispersive ones are rapid data collection, strong signal, large signal-to-noise ratio, and less sample heat-up (Dolgaev *et al.*, 2002). Further advancement has been made in an FTIR method called attenuated total reflection (ATR)-FTIR spectroscopy (Iravani *et al.*, 2014). Using ATR-FTIR, it can determine the chemical properties on the polymer surface, and sample preparation is easy compared to conventional FTIR (Tsuji *et al.*, 2003). Therefore, FTIR is a suitable, valuable, non-invasive, cost effective, and simple technique to identify the role of biological molecules in the reduction of nanoparticles.

2.8.5 X-ray Photoelectron Spectroscopy (XPS)

X-ray is a quantitative spectroscopic surface chemical analysis technique used to estimate empirical formulae (Iravani *et al.*, 2014). XPS is also known as electron spectroscopy for chemical analysis (ESCA), (Kalishwaralal, 2010). XPS plays a unique role in giving access to qualitative, quantitative/semi-quantitative, and speciation information concerning the sensor surface (Iravani *et al.*, 2014). XPS is performed under high vacuum conditions. X-ray irradiation of the nanomaterial leads to the emission of electrons, and the measurement of the kinetic energy and the number of electrons escaping from the surface of the nanomaterials gives XP spectra (Chen *et al.*, 2014). The binding energy can be calculated from kinetic energy. Specific groups of starburst macromolecules such as P=S, aromatic rings, C–O, and C=O can be identified and characterized by XPS (Iravani *et al.*, 2014).

2.8.6 Scanning electron microscopy (SEM)

Recently, the field of nanoscience and nanotechnology has provided a driving force in the development of various high-resolution microscopy techniques in order to learn more about nanomaterials using a beam of highly energetic electrons to probe objects on a very fine scale (Dang *et al.,* 2012). Among various electron microscopy techniques, SEM is a surface imaging method, fully capable of resolving different particle sizes, size distributions, nanomaterial shapes, and the surface morphology of the synthesized particles at the micro and nanoscales (Iravani *et al.,* 2014). Using SEM, the morphology of particles and derive histogram from the images by either by measuring and counting the particles manually, or by using specific software can be probe . The limitation of SEM is that it is not able to resolve the internal structure, but it can provide valuable information regarding the purity and the degree of particle aggregation. The modern high-resolution SEM is able to identify the morphology of nanoparticles below the level of 10 nm.

2.8.7 Transmission electron microscopy (TEM)

Transmission Electron Microscopy is a valuable, frequently used, and important technique for the characterization of nanomaterials, used to obtain quantitative measures of particle and/or grain size, size distribution, and morphology (Rudra *et al.,* 2014). The magnification of TEM is mainly determined by the ratio of the distance between the objective lens and the specimen and the distance between objective lens and its image plane (Wang *et al.,* 2012). TEM has two advantages over SEM: it can provide better spatial resolution and the capability for additional analytical measurements. The disadvantages is that it required high vacuum, thin sample section (Pandy *et al.,* 2012) and the vital aspect of TEM is that sample preparation is time consuming. Therefore,

sample preparation is extremely important in order to obtain the highest-quality images possible.

2.8.8 Atomic force microscopy (AFM)

Generally, AFM is used to investigate the dispersion and aggregation of nanomaterials, in addition to their size, shape, sorption, and structure; three different scanning modes are available, including contact mode, non-contact mode, and intermittent sample contact mode (Basar *et al.,* 2012). AFM can also be used to characterize the interaction of nanomaterials with supported lipid bilayers in real time, which is not achievable with other electron microscopy (EM) techniques. In addition, AFM does not require oxide-free, electrically conductive surfaces for measurement, does not cause appreciable damage to many types of native surfaces, and it can measure up to the sub-nanometer scale in aqueous fluids (Chou *et al.,* 2004). However, a major drawback is the over estimation of the lateral dimensions of the samples due to the size of the cantilever (Sun *et al.,* 2008). Therefore, much attention has to be provide to avoid erroneous measurements (Chanda *et al.,* 2011). Furthermore, the choice of operating mode—no contact or contact—is a crucial factor in sample analysis (Palu *et al.,* 2008).

2.8.9 Localized surface plasmon resonance (LSPR)

LSPR is a coherent, collective spatial oscillation of the conduction electrons in a metallic nanoparticle, which can be directly excited by near-visible light. The localized surface Plasmon resonance (LSPR) condition is defined by several factors, including the electronic properties of the nanoparticle, the size and shape of the particle, temperature, the dielectric environment, and so on (Wang *et al.,* 2012). Small changes in the local dielectric environment cause the dysfunction of LSPR. The frequency of the LSPR spectral peak is very sensitive to the nanostructure environment through the local refractive index. Thereby, shifts of the LSPR frequency are widely used as a method for

the detection of molecular interaction close to the surface of the nanoparticle (Wang *et al.,* 2012). In addition, the near-field enhancement has led to a very large variety of advances in many fundamental and applied areas of science, particularly for the determination of nanoparticle shapes, dimensions, and compositions. This spectroscopy method is being used to investigate fundamental properties and processes of nanoparticles in (bio)-molecular detection devices, or (bio)-imaging tools with improved single-molecule sensitivity. LSPR spectroscopy can provide thermodynamic and real-time kinetic data for binding processes. LSPR-based tools is helpful to analyze faster and with higher sensitivity. The application of LSPR spectroscopy is mainly used for biological and chemical sensing by transducing changes in the local refractive index via a wavelength-shift measurement, due to its sensitivity, wavelength tunability, smaller sensing volumes, and lower instrumentation cost. Single-nanoparticle LSPR spectroscopy is an important tool for understanding the relationship between local structure and spectra. In addition, single nanoparticles can provide higher refractive-index sensitivity than nanoparticle arrays (Wang *et al.,* 2012).

2.9 Green Synthesis of Zinc Oxide Nanoparticles

2.9.1 Plant-mediated biosynthesis of ZnO NPs.

ZnO NPs are known to be multifunctional inorganic nanoparticles with many applications. *Vitex negundo* plant extract was used to produce ZnONPs with zinc nitrate hexahydrate as a precursor. i.e biosynthesized ZnO NPs showed antimicrobial activities against *E. coli* and *S. aureus* bacteria (Chou *et al.,* 2004). Dobrucka and Dugaszewska (2017) used *Trifolium pratense* to synthesize ZnO NPs. i.e synthesized ZnO NPs were found to be of hexagonal shape and the sizes were found to be of 60–70 nm. Kalpana *et al*., (2011) synthesized ZnO NPs using *Lagenariasiceraria* pulp extract. In addition, the author evaluated the biosynthesized ZnO nanoparticles for antidandruff, antimicrobial,

and antiarthritic efficacy. Dhanemozhi *et al.* (2009) successfully synthesized the ZnONPs from green tea leaf extract to evaluate their capacitance behavior for supercapacitor applications. Santhoshkumar *et al.* (2014) synthesized the ZnO NPs using *Passiflora caerulea* leaf extract and tested against the pathogenic culture isolated from the urine of the patient suffering from urinary tract infection. Hussein *et al.* (2010) reported Bacillius cereus as a biotemplate agent for the formation of ZnO NPs with raspberry and plate-like structures through a simple thermal decomposition of zinc accate maintiaing the original pH of the reaction mixtures.

2.9.2 Plant description (*Senna occidentalis* Linn)

Senna occidentalis L. commonly known as coffee senna is distributed as a weed throughout the tropical and subtropical regions of the world. It can be found at low and medium altitudes as a weed in waste places, in open pastures and in fields cultivated with economic crops such as soybean, cotton, corn, sorghum etc. It grows luxuriantly in all available spaces, such as neglected gardens, roadsides, near lakes or streams and unused grounds of public buildings (Stevens *et al*., 2001; Vashishtha *et al*., 2009). In West of Africa, *Senna occidentalis* seeds are commonly roasted and infused in a coffee-like beverage.

The plant's tissues of *Senna occidentalis* contain a host of phytoactive chemicals that may support its numerous applications in folk medicine. Extracts or powdered leaves are used as an analgesic, antibacterial, antifungal, anti-inflammatory, antiseptic, antispasmodic, antiparasitic, antiviral, diaphoretic, insecticidal, laxative, purgative etc (Raintree, 2002). It is also used against stomach disorders, rheumatism and in treatment of liver diseases. The leaves and roots are ingredients of many popular herbal tonics, medicines for liver and stomach disorders. The seeds of coffee senna are roasted and used as a coffee substitute and the leaves are widely used as a leafy vegetable and eaten

either raw or mixed with coconut, chilli and onion (Selvam, 2007; Vashishtha *et al*., 2009).

Phytochemicals contained in plant foods have been linked to many positive effects on human health, including coronary heart diseases, diabetes, high blood pressure, cataracts, degenerative diseases and obesity (Liu *et al*., 2010).

Coffee *Senna* is a weed grown naturally in the wild which is rich in proteins, lipids, carbohydrates, calcium, iron, trace of caffeine and because of its little or no potential uses, a massive volume of this species has been wasting away which could have been harnessed for human uses.

Plate I: *Senna occidentalis* (Source: Vashishtha *et al.*, 2009)

CHAPTER THREE

3.0 MATERIALS AND METHODS

3.1 Materials

3.1.1 Plant materials:

Fresh leaves of *Senna occidentalis* were collected from Bosso Local Government Area, Niger State, Nigeria by 10.00 am on the 23rd of July, 2019.

3.1.2 Reagents:

All the chemicals that were used were of analytical grade. Silver trioxonitrate (v) salt, Zinc Acetate dihydrate, aluminum chlorides, hydrochloric acid, sodium hydroxide, iron s(III) chloride, concentrated ammonium hydroxide, methanol and concentrated sulphuric acid.

3.2 Methods

3.2.1 Sample preparation

The leaves were washed properly with distilled water, shade dried and then pulvenized into coarse powder using a blender. *Senna occident*ali aqueous extract were prepared by weighing 20 g of the coarse powder in 400 mL of distilled water in a conical flask and heated in a water bath under constant shaking at 60˚C for 50 minutes. The extract were filtered using whatman No 1 filter paper and the filtrate were stored at 40˚C in order to prevent fermentation for further use. (Sivakumar *et al.*, 2014).

3.2.2 Qualitative phytochemical screening

Quantitative phytochemical components of were determined according to the method described by AOAC (1999) to confirm for the presence of alkaloids, saponins, flavonoids, cardiac glycosides, tannins, steroids, phlobatannin, terpenoids and anthraquinones.

3.2.2.1 Test for alkaloids

Presence of alkaloids in the sample was determined according to the method described by Harborne (1973) which, 0.2 g of the sample was boiled with 5 mL of 2 % HCl on a steam bath. The mixture was filtered and 1 ml portion of the filtrate was treated with 2 drops of dragendorff's reagent: A red precipitate indicated the presence of alkaloids.

3.2.2.2 Test for flavonoids

Presence of Flavonoids in the sample was determined according to the method described by Chang *et al*., (2013). In a test tube, 0.2 g of the sample was heated with 10 mL ethyl acetate in boiling water for 3 minutes. The mixture was filtered off and the filtrate was used for ammonium test: about, 4 mL of the filtrate was shaken with 1mL of dilute ammonium solution. The layers were allowed to separate. And a yellow precipitate observed at the ammonium layer indicated the presence of flavonoids.

3.2.2.3 Test for saponins

Presence of saponins in the sample was determined by the method described by Oloyede, (2005). In a test tube, 0.1 g of the sample was boiled with 5mL of distilled water for 5 minutes. The mixture was filtered. The filtrate was used for Frothing test: One mixture, 1 ml of the filtrate was diluted with 4 mL of distilled water. The mixture was shaken vigorously and then observed on standing for a stable froth.

3.2.2.4 Test for tannins

The presence of tannins in the sample was determined by the method described by Harborne (1973). In a test tube, 2 g of the sample was boiled with 5 mL of 45 % ethanol for 5 minutes. The mixture was cooled and then filtered. The filtrate was treated with ferric chloride solution: about 1 mL of the filtrate was diluted with distilled water and then 2 drops of ferric chloride solution was added. A transient greenish to black colour indicated the presence of tannins

3.2.2.5 Test for phenolic compounds

The presence of phenol in the sample was determined by the method reported by Singleton *et al*. (1999). The extract (50 mg) is dissolved in 5 mL of distilled water and few drops of 5 % ferric chloride solution were added. A dark green colour indicates the presence of phenolic compound.

3.2.2.6 Test for anthraquinones

The plants extract was shaken with equal volume of 10 % ammonia solution added to chloroform layer. Formation of a brick red precipitate indicates the presence of anthraquinones.

3.2.2.7 Test for terpenoids

Extract 5 ml was mixed with 2 millitres of chloroform in a test tube and 3 mL of Conc H_2SO_4 was carefully added to the mixture to form a layer. An interface with redish brown colouration is formed if terpenoids constituent is present.

3.2.2.8 Cardiac glycosides

Two grams (2.0 g) of the extract was mixed with 30 mL of distilled water in a test tube and sheated in a water bath for 5 minutes. The mixture was filtered and 5 ml of the filtrate was added to 0.3 ml of Fehling's solutions A and B until it turned alkaline (tested with litmus paper) and heated on a water bath for 2 minutes. A brick-red precipitate indicated the presence of glycosides according to the method described by Trease and Evans (1983).

3.3 Synthesis of ZnO Nanoparticles

Zinc oxide nanoparticles were synthesized by green synthesis method using Zinc acetate salt and aqueous extract of *Senna occidentalis*. 200 mL of distilled water were added to 20 g of zinc acetate followed by heating on a water bath for 2 minutes and stirred at 50 rpm using a magnetic stirrer, 50 mL of the plant extract were added and the solution of

NaOH (pH 11) was also added, a yellowish precipitate was obtained. Then the solution was allowed to age for 24 h in an oven of 45 ˚C. After which the solution sediment and clear solution obtained was decanted followed by washing of the residue and subsequent calcination at temperatures 400 for 1h, 500 for 2h and 650 for 1h a white residue was obtained which was pulverized into powered form.

3.3.1 Green synthesis of silver nanoparticles

Aqueous extract of *Senna occidentali* (5 ml) was added to 95 ml of aqueous solution of 1mM silver nitrate $AgNO_3$and heated with stirrer at 70 ˚C for 60 minutes and pH 7 (Aja *et al.*, 2010).

3.3.2 Optimization of silver nanoparticles

To improve the optimization of the central composite design of experiments (one factor-at-a time method) was used, the factors to be considered were concentration of Silver nitrate (1mM), 7.5 mls of leaf extract, temperature (65 ^oC), pH (6.5) and time (50 minutes). (Aja *et al.*, (2010).

3.3.3 Characterization

3.3.3.1 UV-visible spectral analysis

UV visible spectrum were evaluated using UV-spectrophotometer with a wavelength range of 200-800 nm for ZnONps and AgNps (Patil *et al.*, 2016). UV- Visible spectral analysis is based on the absorption of ultraviolet or visible light by chemical compounds, which results to the production of distinct spectral.

3.3.3.2 Particle size

Size were evaluated by zeta silver instrument (Malvern Zetasizer Nano zs90) and the results was acquired by the nano software (Singh *et al.*, 2013). Malvern Zetasizer uses the principle of static light scattering (SLS), SLC measure absolute molecular weight

using the relationship between the intensity of light scattered by the nanoparticles and it molecular weight and size.

3.3.3.3 Fourier transform infra-red (FTIR) analysis: Fourier transform infra-red (FTIR) analysis of the NPs (nano particles) were carried out with fourier transform spectrometer as described by (Singh *et al*., 2013). The principle is that molecular vibration takes places as a result of absorption of infrared radiation.

3.3.3.4 Transmission electron microscopy (TEM): The morphology and the mean size of synthesized AgNps and ZnONps were measured using electron microscope (Zawrah *et al*., 2013). The principle is that beam of electrons is passed through a sample to produce an image.

3.3.3.5 X- Ray Diffraction Analysis (XRD)

The average crystallite size of the synthesized nanoparticles (zincite) were calculated using Debye-Scherrer as presented in equation 4.1:

$$D = \frac{k\lambda}{B\cos\theta} \qquad (4.1)$$

Where D is the crystallite size (nm), k is a constant (0.94 for spherical particles), λ is the wavelength of the X-ray radiation (CuKaα = 0.1541 nm), β is the full width at half maximum (FWHM) of the intense and broad peaks and θ is the Bragg's or diffraction angle.

Standard procedures described by AOAC (1984), Sofowara (1993), Harborne (1998), Oloyed (2005).

3.4 Antibacterial Assay of doped and Undoped Silver and Zinc Oxide nanoparticles

3.4.1 Reconstitution of Nanoparticles (AgNps, ZnONps and Doped Zn/ Ag Nps)

The reconstitution of the AgNps, 1mL of 1.0 Mm of AgNps solution were dissolved in 4mL distilled water to make up 5 mL AgNps (stock solution) to get concentrations of

20, 40 and 60 mg/mL, 0.1,0.2 and 3 mL respectively were taken from the stock solution to get each concentrations .

The reconstitution of the ZnONps, to get concentrations of 20, 40 and 60 mg/mL, 0.02, 0.04 and 0.06 g of the ZnONps were dissolved in 1 ml of DMSO and 4 mL distilled water.

The preparation and reconstitution of the Doped ZnO/ AgNps, 5 ml of 1 mM AgNps was added to 5 mL of 1 Mm ZnONps, 10mL of distilled water to make up 20 mL of Doped ZnO/AgNps, the final product is kept under constant stirring for 6h. The final product is allowed to settle, the product (stock solution) to get concentrations of 20, 40 and 60 mg/mL, 0.1, 0.2 and 3ml respectively were taken from the stock solution to get each concentrations.

3.4.2 Sources of microorganisms

The four bacteria isolates assayed in this study were *Escherichia coli, Staphylococcus aureus, Strephococcus pyogenes and Pseudomonas aeruginosa.* These organisms were obtained from the Centre for Genetic Engineering and Biotechnology, Federal University of Technology, Minna, Niger State. Mueller Hinton Agar was used to confirm the organisms by sub-culturing at 37 °C for 18 hours; and the organisms were maintained in a refrigerator at 4 °C until required as described by (Igbinosa *et al*., 2009).

3.4.3 Preparation of media

Twenty-eight grams of Mueller Hinton agar (standard measurement) was poured into sterile conical flask; to which 1 litre of distilled water was added to the conical flask. The prepared media were cork-fitted with cotton wool, foil paper, and masking tape. This was done to avoid removal of the cork when autoclaving. The media was

autoclaved for 15 minutes at 121 °C, removed and cooled to 47 °C. It was then pr Subsequently, these were mixed properly before pouring into sterile petri-dishes.

3.4.4 Standardization of inoculum

Three colonies of test organisms were picked, inoculated into 5 mL of sterile Mueller Hinton Agar and incubated (18-24 hrs) for bacterial growth. Turbidity was adjusted to match 0.5 McFarland's standard (Coyle, 2005).

3.4.5 *In vitro* evaluation of antibacterial activity

The extracts of the leaf extracts *Senna occidentalis* were evaluated *in vitro* for antibacterial activity against *Staphylococcus aureus*, and *Escherichia coli, Pseudomonas aeruginosa, Strephococcus pyogenes* 1.0 Mm $AgNO_3$, 1.0 mM Zinc acetate dihydrate and Amoxicillin were used as the control, Nutrient agar (28 g) was added to 1 litre distilled water in a conical flask. This was stirred and autoclaved at 121°C and then cooled to 50°C. A portion of the medium (20 mL) was poured into a sterile Petri dish and allowed to solidify. The sterility of the medium was confirmed by allowing it to stay for 8 hrs and ensuring no contamination (Daniyan *et al*., 2011).

An isolate colony of each test organism was sub-cultured on Nutrient agar and incubated at 37°C for 8 h. This was spread on the entire plate medium to ensure uniform growth. Sterilized crude extract for agar well diffusion method. It was placed inside the bored holes on the agar plates containing the test organisms. The plates were, subsequently, incubated for 24 h at 37°C (Wakirwa *et al*., 2013). Zones of inhibition were observed using a hand lens for proper magnification and measured. Antimicrobial assays were carried out in triplicate'

3.4.6 Minimum Inhibitory Concentration (MIC) of the Nanoparticles

The MIC of nanoparticles against the test organisms were determined using the broth dilution method as described by the NCCLS (2003). Briefly, 4 ml of Mueller Hinton

Agar was dispensed into three test tubes and autoclaved for 15 minutes. Two point five millilitre of stock solutions of the nanoparticles (AgNps, ZnONps and Doped ZnO/ AgNps) at the concentration of 40 mg/ml each of the nanoparticles were added to the test tube, and serial diluted to obtain concentrations of 20,10,5,2.5 mg/mL of each of the nanoparticles were made. A loopful of standardized test organisms adjusted to 0.5 McFarland standard was inoculated into each tube. Positive controls were equally set up by using the Mueller Hinton Agar alone and the nanoparticles test tubes were sealed with foil paper, cotton wool, and masking tape.

The tubes were then incubated at 37°C for 18-24 hrs. Tube (s) with least concentration or with no detectable growth when checked visually for turbidity was recorded as the MIC (Abalaka *et al.,* 2011).

3.4.7 Minimum Bactericidal Concentration (MBC) of the nanoparticles (AgNps, ZnONps and Doped ZnO/ AgNps)

Sample from the tubes used in MIC determination, which did not show any visible growth after period of incubation, were streaked out on Nutrient Agar for 24 hrs to determine the minimum bactericidal concentration of the extract that will kill the test organisms. The lowest concentration of the extract indicating a bactericidal effect after incubation was regarded as the Minimum Bactericidal Concentration (MBC) (Aboada *et al.,* 2006).

3.4.8 Data Analysis

One-way analysis of variance (ANOVA) was used to compare the mean differences between the zones of inhibition of the extracts and controls. Significant difference between means were separated by Duncan multiple range test (DMRT). All results were expressed as mean±SD, while all statistical decisions were taken at 95 % level of significance.

CHAPTER FOUR

4.0 RESULTS

4.1 Phytochemical Composition

The qualitative phytochemical constituents of aqueous extracts of *Senna occidentali* is presented in Table 4.1. The qualitative phytochemical constituents of aqueous extract of *Senna occidentalis* revealed the presence of alkaloids, flavonoids, tannins, anthraquinones, phenols, terpenoids, glycosides and saponins respectively.

Table 4.1: Phytochemical Constituents of Aqueous Extract of *Senna occidentalis*

Phytochemical	Inference
Alkaloids	+
Flavonoids	+
Tannins	+
Anthraquinones	+
Phenols	+
Terpenoids	+
Cardiac Glycosides	+
Saponins	+

Keys: = (+) Present, (-) Absent

4.2 Effect of Reaction of pH on Zinc Oxide Nanoparticles (ZnONps)

4.2.1 Effect of reaction at pH 7 on Zinc Oxide nanoparticles (ZnONps)

The result of the effect of reaction at pH 7 on Zinc Oxide nanoparticles (ZnONps) is presented in Figure 4.1. Zinc oxide nanoparticles synthesized using pH at 7 showed absorbance at wavelength of 329 nm is presented in Figure 4.1, other minimal peaks were at 300, 275 and 250nm.

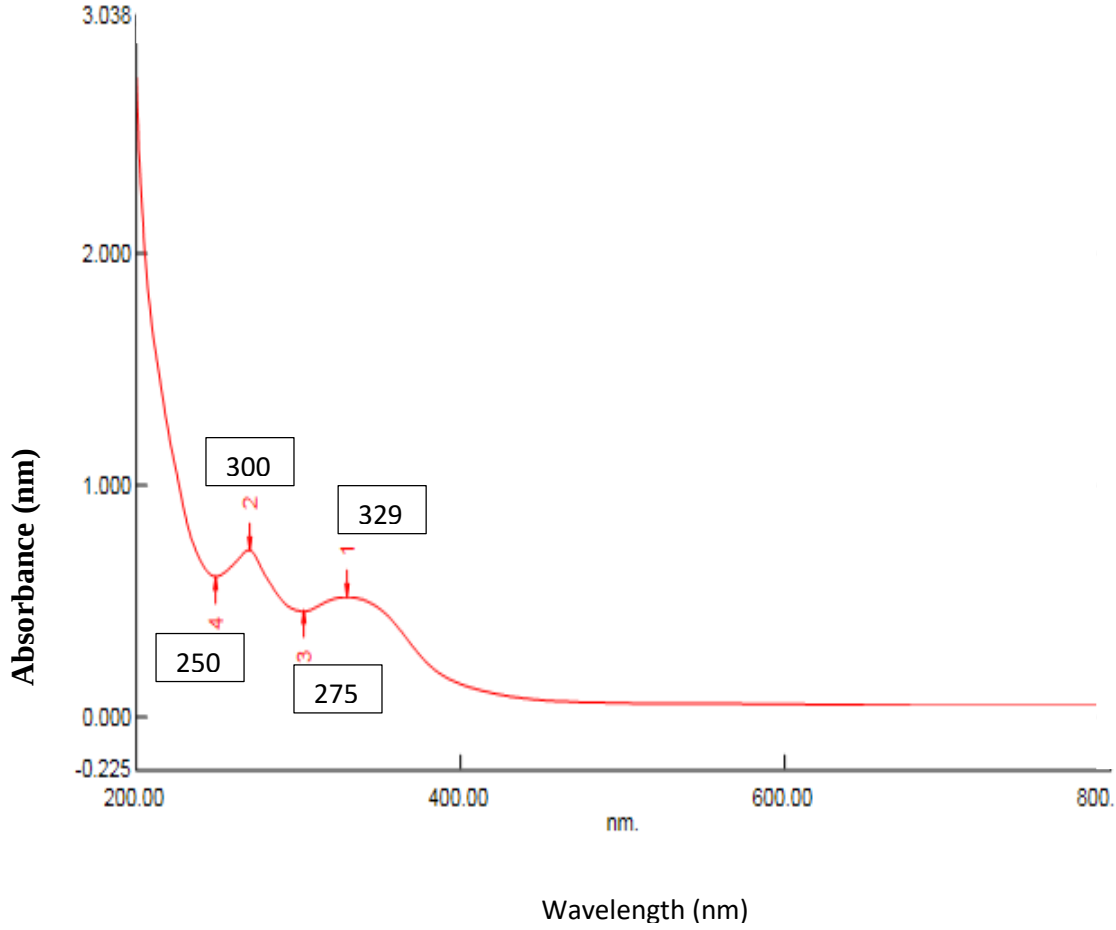

Figure 4.1: Effect of Reaction at pH 7 on Zinc Nanoparticle Synthesized with *Senna occidentalis*

4.2.2 Effect of reaction at pH 10 on Zinc Oxide Nanoparticles (ZnONps)

The result of effect of reaction at pH 10 on Zinc oxide Nanoparticles (ZnONps) is presented in Figure 4.2. Zinc nanoparticles syngthesized at pH 10 showed absorbance at wavelength 393 nm presented in Figure 4.2, other minimal peaks were at 320, 295, 350 and 300nm.

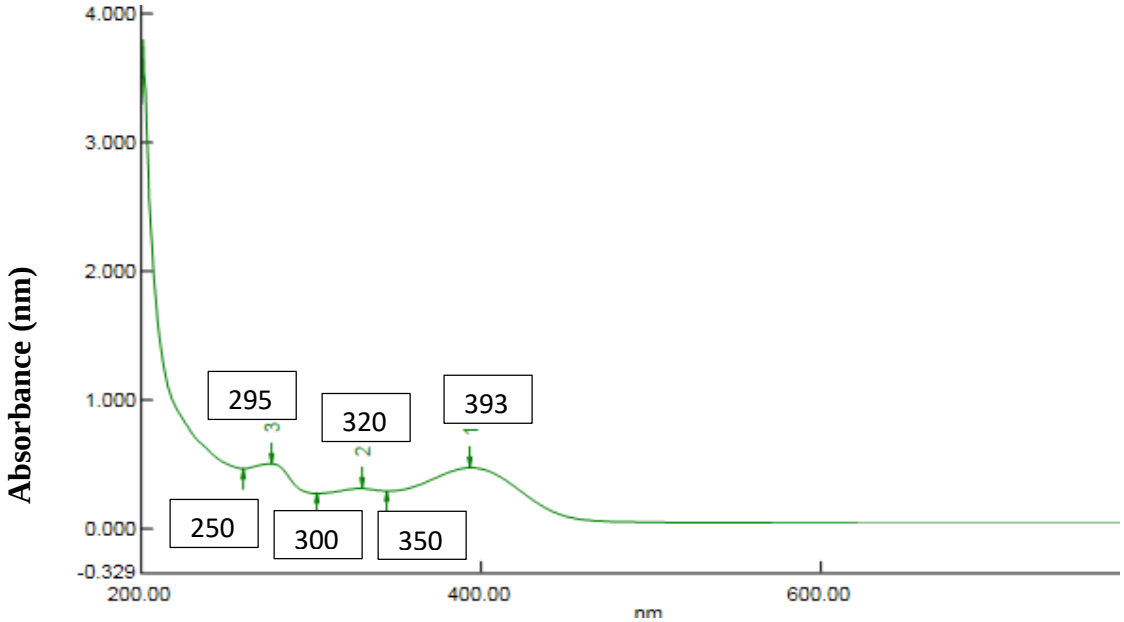

Figure 4.2: Effect of Reaction at pH 10 on Zinc Nanoparticle Synthesized with *Senna Occidentalis*

4.2.3 Effect of reaction at pH 11 on Zinc Oxide Nanoparticles (ZnONps)

The result of effect of reaction at pH 11 on Zinc oxide nanoparticles (ZnONps) is presented in Figure 4.3. Zinc oxide nanoparticles synthesized using pH 11 showed absorbance at wavelength of 393 nm presented in Figure 4.3, other minimal peaks were at 320, 295, 350, 300 and 250nm.

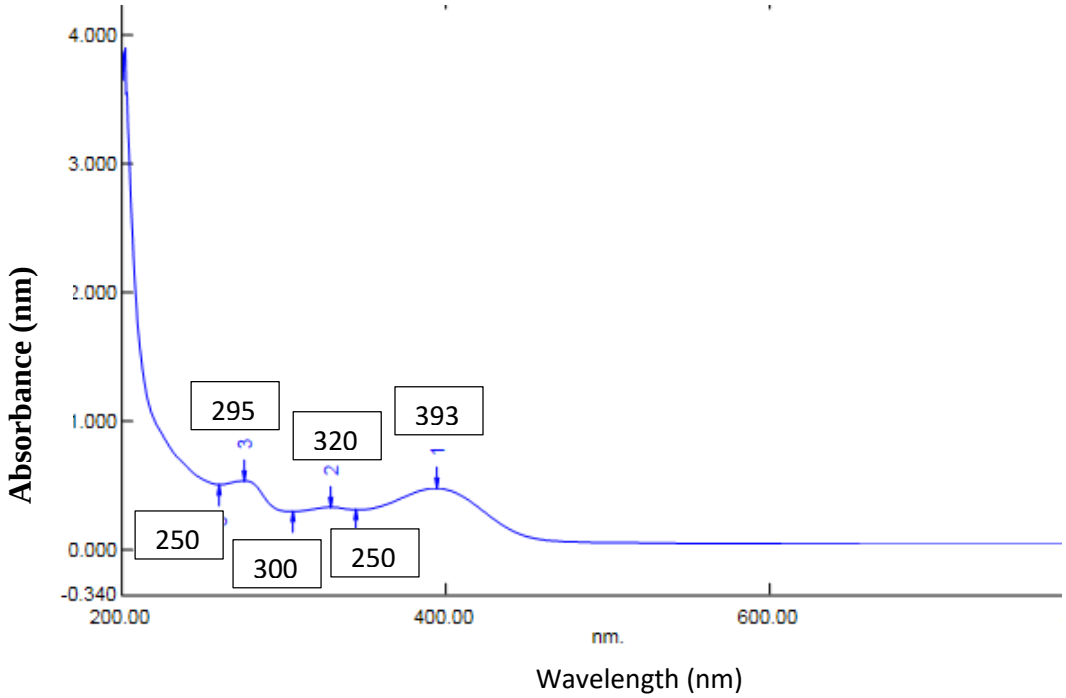

Figure 4.3: Effect of Reaction at pH 11 on Zinc Nanoparticle Synthesized with *Senna Occidentalis*

4.2.4 Effect of Reaction of pH 12 on Zinc Oxide nanoparticles

The result of effect of Reaction at pH 12 on Zinc Oxide nanoparticles is presented in Figure 4.4. Zinc oxide nanoparticles synthesized using pH of 12 show absorbance at wavelength of 393 nm. Other minimal peaks were at 320, 295, 350, 300 and 250nm.

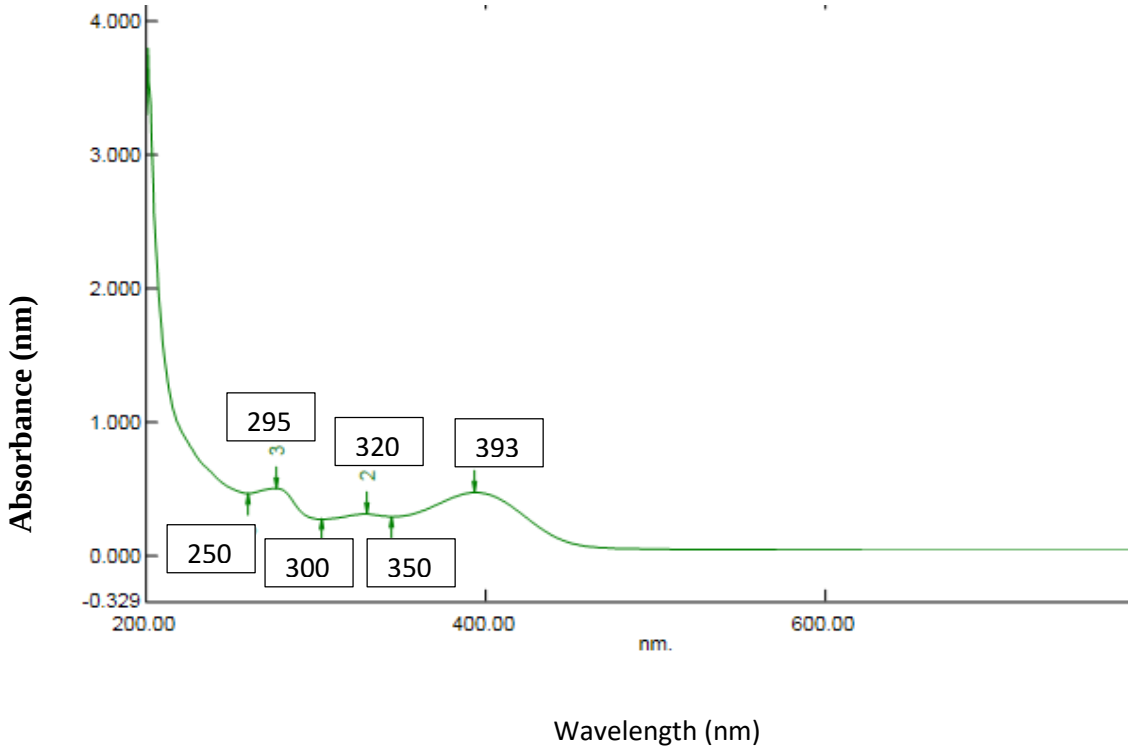

Figure 4.4: Effect of Reaction at pH 12 on Zinc Nanoparticle Synthesized with *Senna occidentalis*

4.3 Particles size of Zinc Oxide Nanoparticles

The result of zeta sizer of Zinc oxide nanoparticle is presented in Figure 4.5. The result showed the particle size distribution of the biosynthesized Zinc Oxide nanoparticles at 52.50 nm at 14 % intensity of 393 nm wavelength.

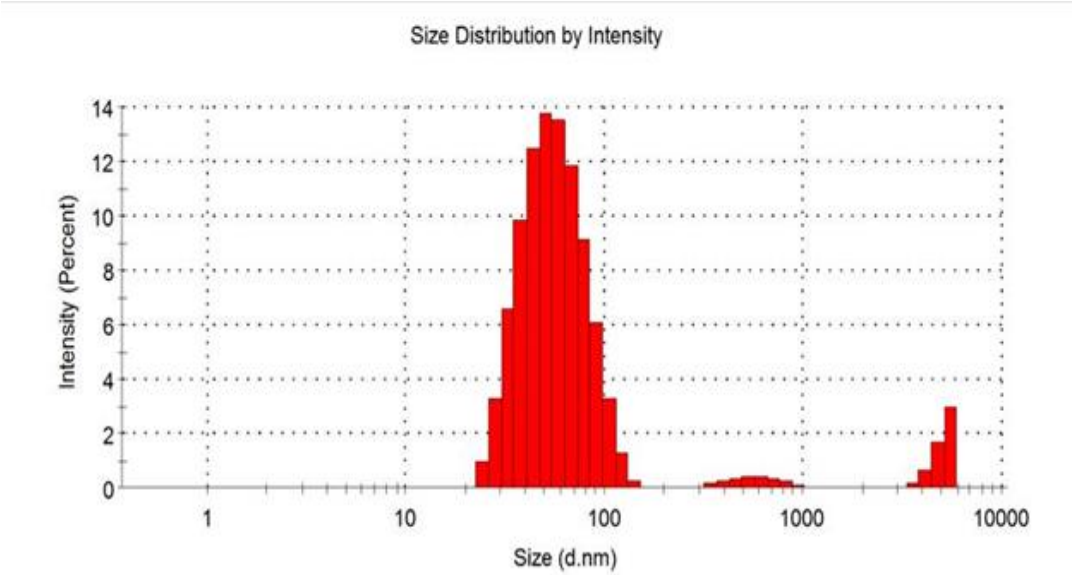

Figure 4.5: Particle Size Diameter of the Biosynthesized Zinc Oxide nanoparticles

4.4 The UV Visible Spectral of Plant Extract and Silver Nanoparticles (AgNps)

The result of UV visible spectral of plant extract and silver nanoparticles (AgNps) in Figure 4.6 The result showed the wave length at which AgNps synthesized at 331 nm at pH 7 and the plant extract *Senna occidentalis* at 334 nm at pH 7.

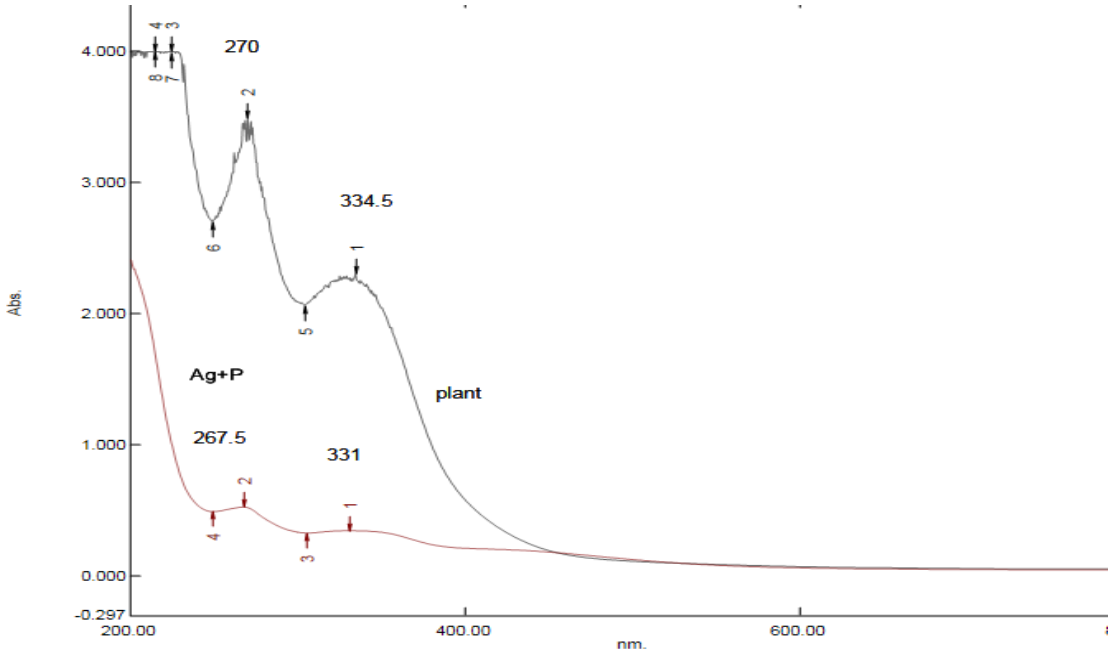

Figure 4.6: Ultraviolet Visible Spectra of Plant Extract and Silver Nanoparticle

4.5 Particles size of Silver nanoparticles

The result of particle zeta sizer of silver nanoparticle is presented in Figure 4.7. The result showed the particles size of distribution of biosynthesized Silver nanoparticles at 83.40 nm with intensity of 14 % at 331 wave length.

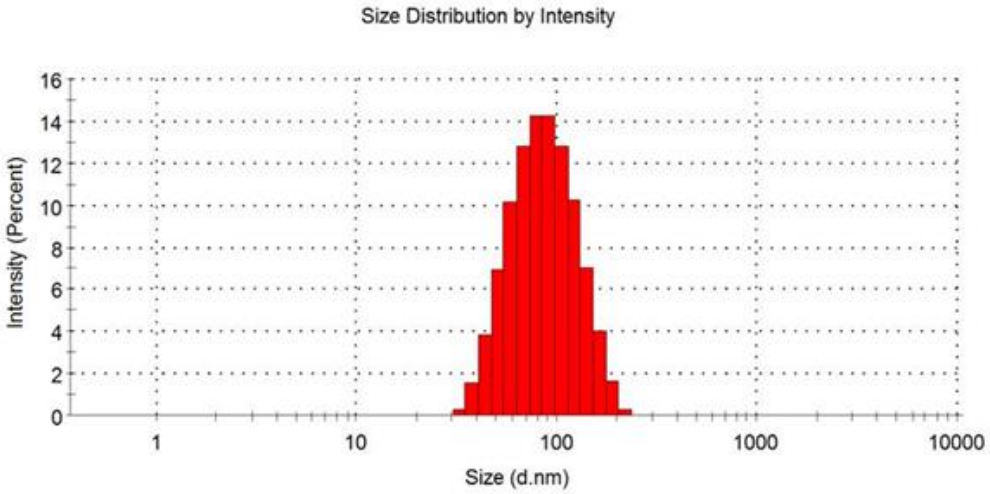

Figure 4.7: Particle size Diameter of the Biosynthesized Silver Nanoparticles Silver Nanoparticles

4. 6 Transmission Electron Microscopy of Bio-synthesized Silver Nanoparticle

The result of transmission electron microscopy of biosynthesized Silver nanoparticles is showed in Plate 2. (A) for 50nm particle (B) for 2nm particle.

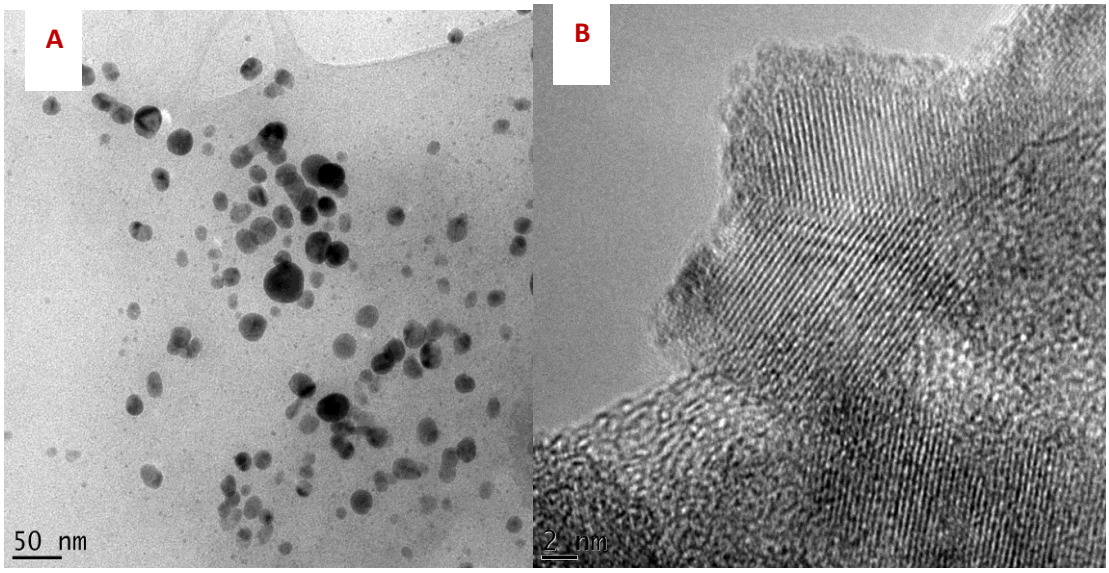

KEY

A	-	**HRTEM- High resolution thermal electron microscope**
B	-	**HRTEM Microscopy**

Plate II: Transmission Electron Microscopy of Bio-synthesized Silver Nanoparticle

4.7 Selected Area Electron Diffraction (SAED)of Biosynthesized Silver Nanoparticles

The result of the selected area electron diffsraction of biosynthesized silver nanoparticles is showed in plate III has a symmetry diffraction spots of 2-1nm

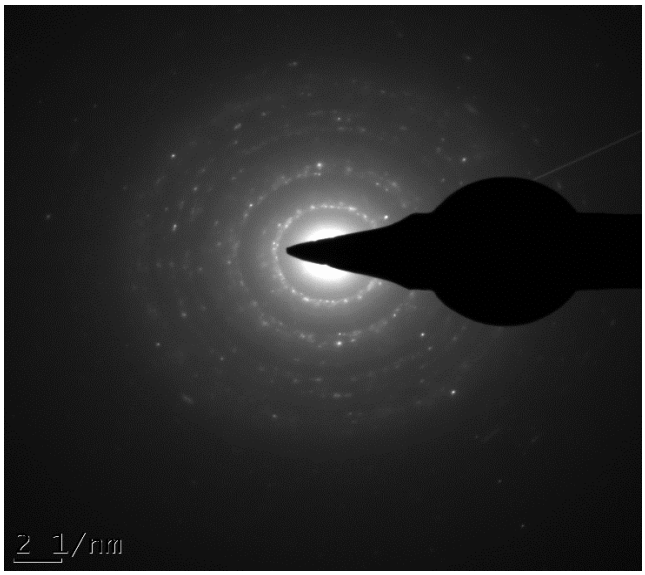

Plate III: SAED (Selected Area Electron Diffraction) of biosynthesized Silver nanoparticles

4.8 Transmission Electron Microscopy of Biosynthesized Zinc Oxide Nanoparticle

The result of transmission electron microscopy of biosynthesized zinc oxide nanoparticle Plate 3 showed (A) the HRTEM for 2nm particle (B) the HRTEM micrography for 20nm particle.

A B

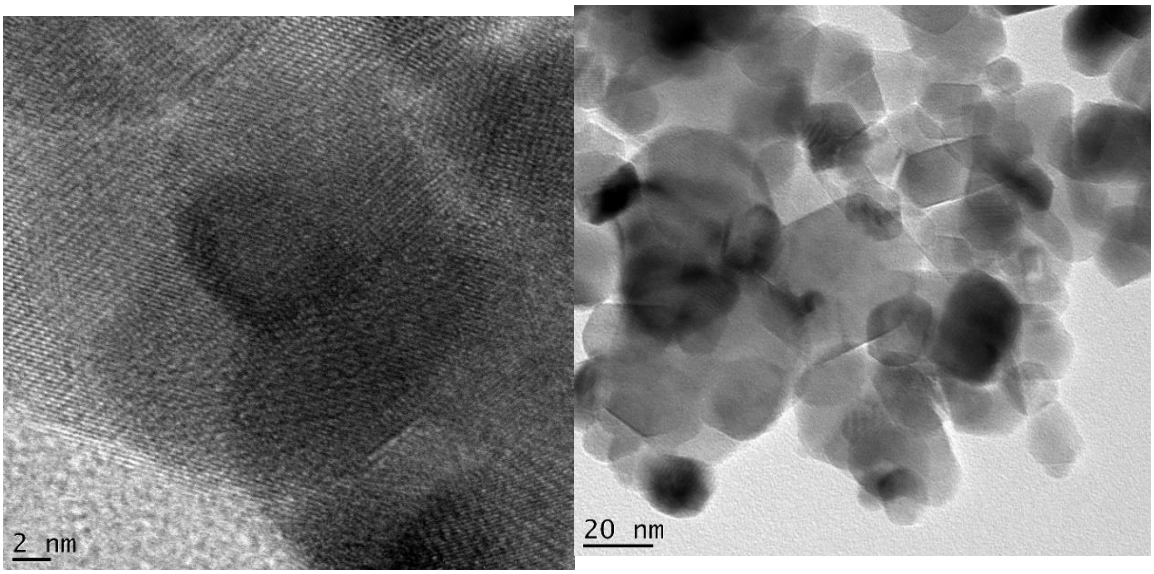

KEY

A	- **HRTEM- High resolution thermal electron microscope**
B	- **HRTEM Microscopy**

Plate IV: Transmission Electron Microscopy of Biosynthesized Zinc Oxide Nanoparticle

4.8 Selected Area Electron Diffraction (SAED) of Biosynthesized Zinc Oxide Nanoparticles

The result of the selected area electron diffraction of biosynthesized zinc oxide nanoparticles is showed in plate V has diffraction rings of 2-1nm, the sharp spot reveals the polycrystalline nature of Zinc oxide nanoparticle

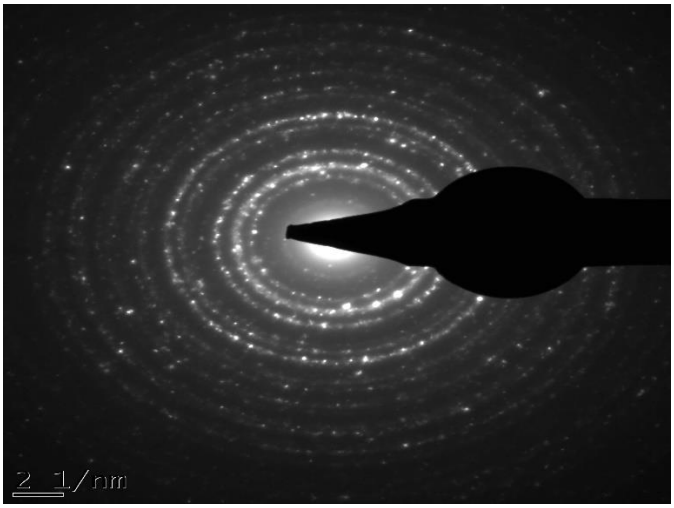

Plate V: SAED (Selected Area Electron Diffraction) of biosynthesized Zinc oxide nanoparticles

4.10 Electron Dispersive Spectroscopy(EDS) of Optimized Biosynthesized Silver Nanoparticles

The result of the electron dispersive Spectral of optimized biosynthesized Silver nanoparticles is presented in Figure 4.8. The optical absorption band peak at Ag 3.0, 3-5 keV, for Copper (Cu) is at 0.9Kev, 1.6kev, 1.8kev, 8.0kev, 9.0kev, for Oxygen (O) is at 0.4kev, for Sodium (Na) is at 1.0kev, for Magnesium (Mg) is at 1.4kev, Silicon(Si) is at 2.0kev; 2.2 kev, for Sulphur(S) is at 3.0kev 3.2kev, Chlorine (Cl) is at 3kev, 3.8kev, Calcium (Ca) is at 3.8kev, 4.0kev, 4.2kev,

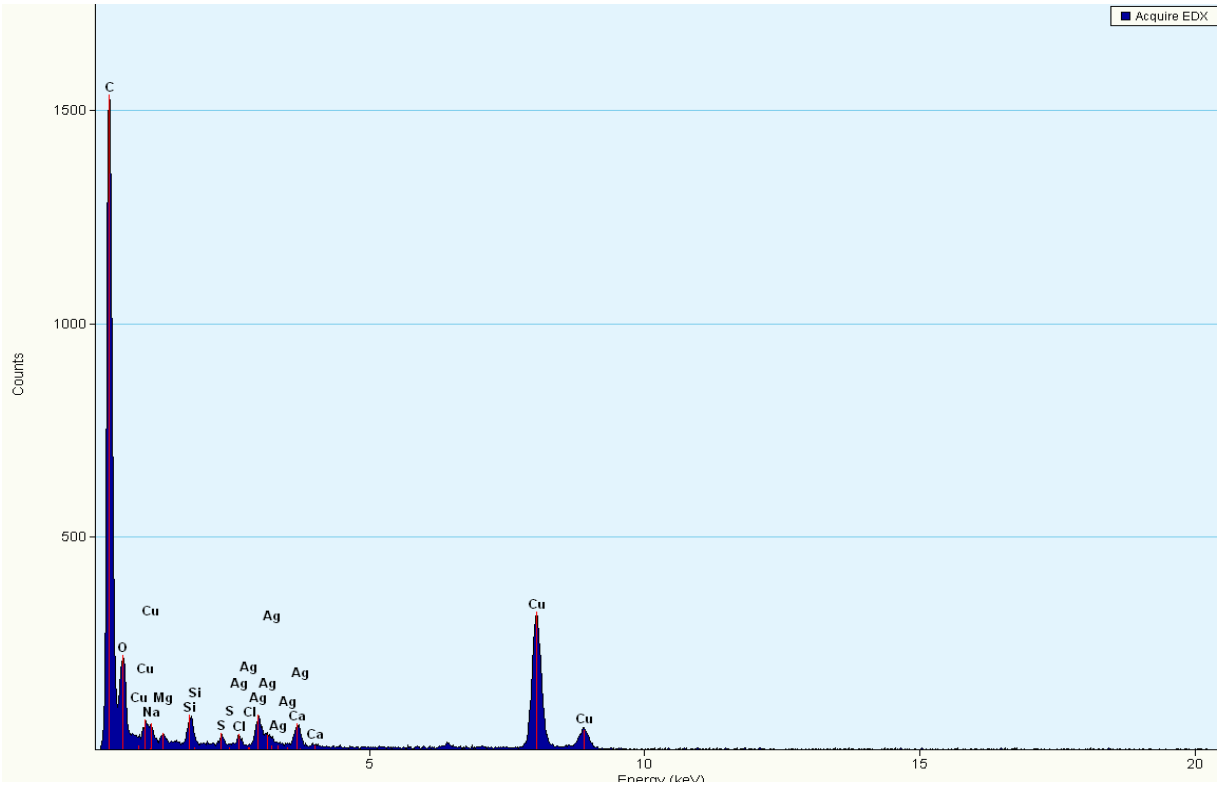

Figure 4.8: Electron Dispersive Spectroscopy (EDS) Spectral of Optimized Bio-synthesized Silver Nanoparticles (SNP)

4.11 Electron Dispersive Spectroscopy (EDS) of Optimized Biosynthesized Zinc Oxide at pH 7

The result of Electron Dispersive spectrum of optimized biosynthesized Zinc oxide nanoparticles synthesized at pH 7 is presented in Figure 4.9. The optical absorption band peak of Zinc (Zn) at 1.0, 8.8 and 9.8 keV and for Carbon (C) at 0.4KeV, for Calcium (Ca) at 0.6 KeV and 3.8KeV, for Oxygen(O) is at 0.8Kev, and for Sodium (Na) at 11.0Kev

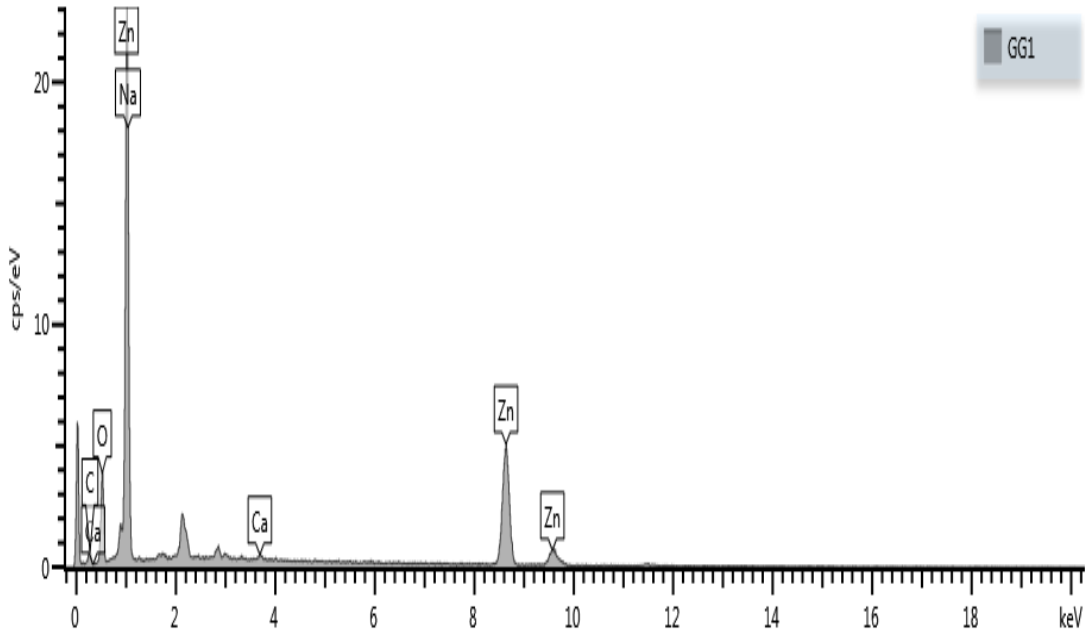

Figure 4.9: Electron Dispersive Spectrum of Optimized Bio-synthesized Zinc Oxide Nanoparticles at pH 7

4.12 Electron Dispersive Spectroscopy (EDS) of Optimized Bio-synthesized Zinc oxide Nanoparticles at pH 10

The result of Electron Dispersive spectral of optimized biosynthesized Zinc Oxide nanoparticles synthesized at pH 10 is presented in Figure 4.10. The optical absorption band peak are of Zinc (Zn) at 1.0, 8.8 and 9.8 keV of Carbon (C) at 0.2keV, of Oxygen(O) at 0.6keV, and Sodium (Na) at 1:0KeV.

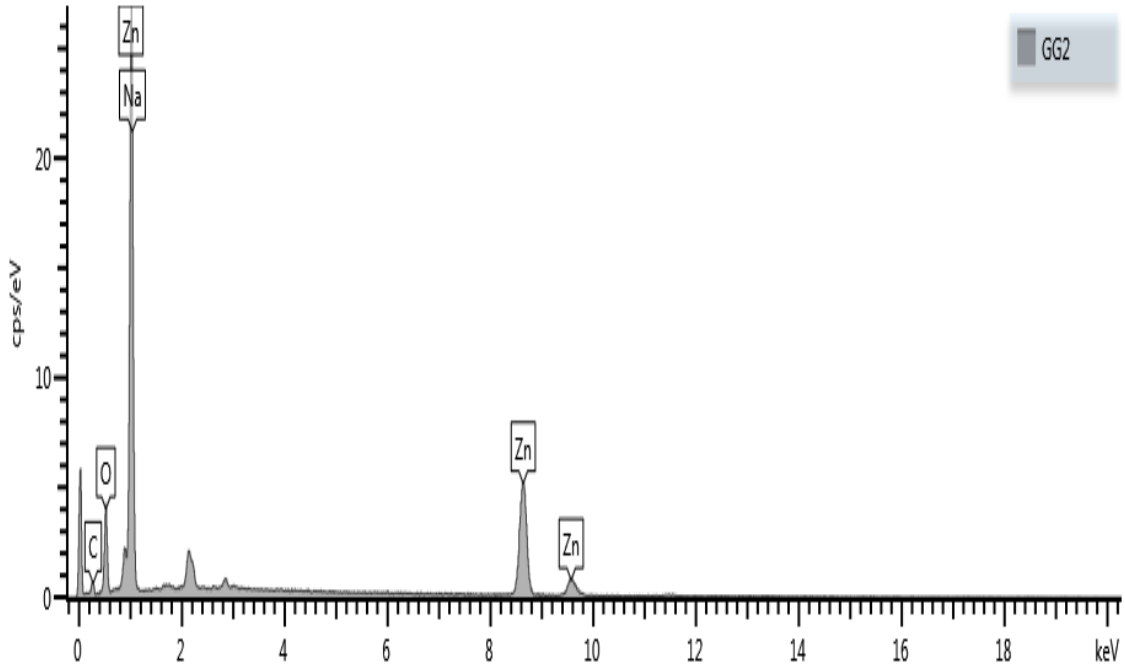

Figure 4.10: Electron Dispersive Spectrum of Optimized Bio-synthesized Zinc oxide Nanoparticles at pH 10

4.13 Electron Dispersive Spectroscopy(EDS) Spectral of Optimized Bio-synthesized Zinc oxide Nanoparticles at pH 11

The result of Electron Dispersive Spectrum of optimized Biosynthesized Zinc oxide nanoparticle synthesized at pH 11 is presented in Figure 4.11. The optical absorption band peaks of Zinc (Zn) are at 1-0, 8,8 and 9.8 KeV for Calcum (Ca) is at 0.42.8, KeV, for Carbon (C) is at 0.4 KeV, for Oxygen (O) is at 0.6 KeV, for sodium (Na) is at 0.8 KeV, and for Silicon (S) is at 0.8 KeV

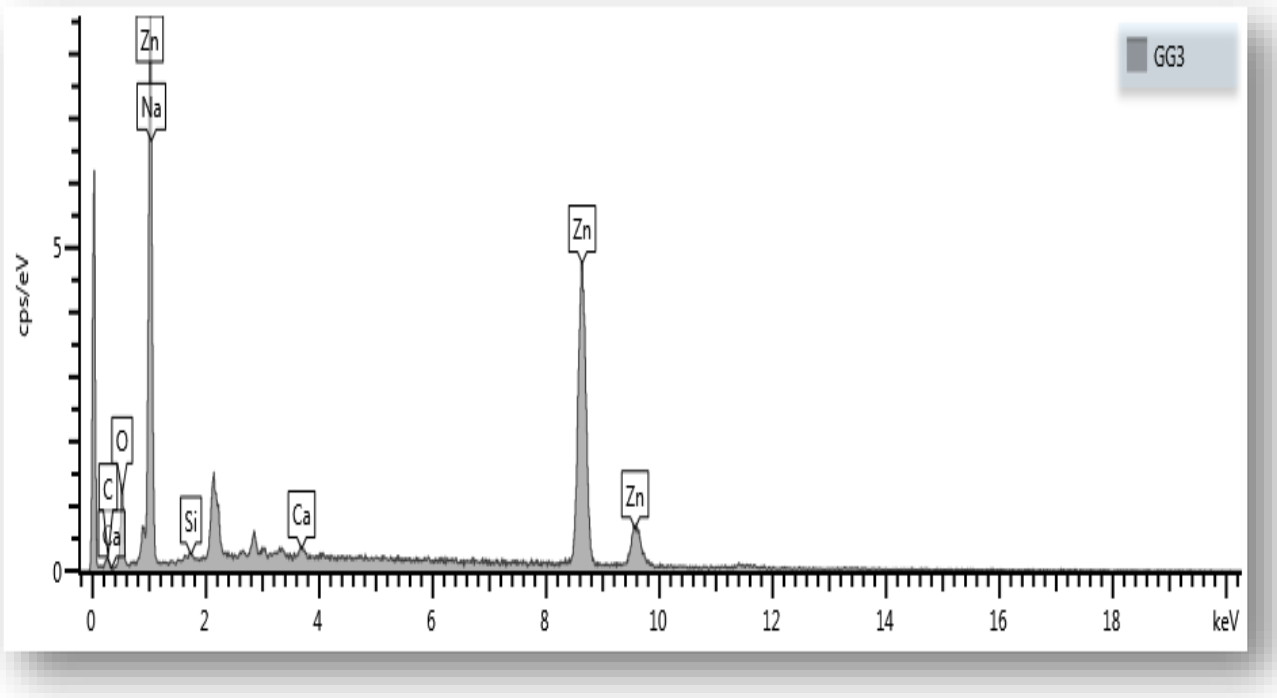

Figure 4.11: Electron Dispersive Spectrum of Optimized Bio-synthesized Zinc Oxide Nanoparticles at pH 11

4.14 Electron Dispersive Spectroscopy(EDS) Spectral of Optimized Bio-synthesized Zinc oxide Nanoparticles at pH 12

The result of Electron Dispersive Spectrum of optimized biosynthesized zinc oxide nanoparticle synthesized at pH 12 is presented in Figure 4.12. The optical absorption band peak of Zinc (Zn) at 1.0, 8.4 and 8.8 KeV, for Calcium (Ca) is at 0.4 and 2.8 KeV, for Carbon (C) at 0.4 KeV, for Oxygen (o) is at 0.6KeV, for Sodium (Na) is at KeV, for Magnesium (Mg) is at 1.4KeV, for Silicon(s) at 1.8keV and for Potassium (K) is at 2.6KeV.

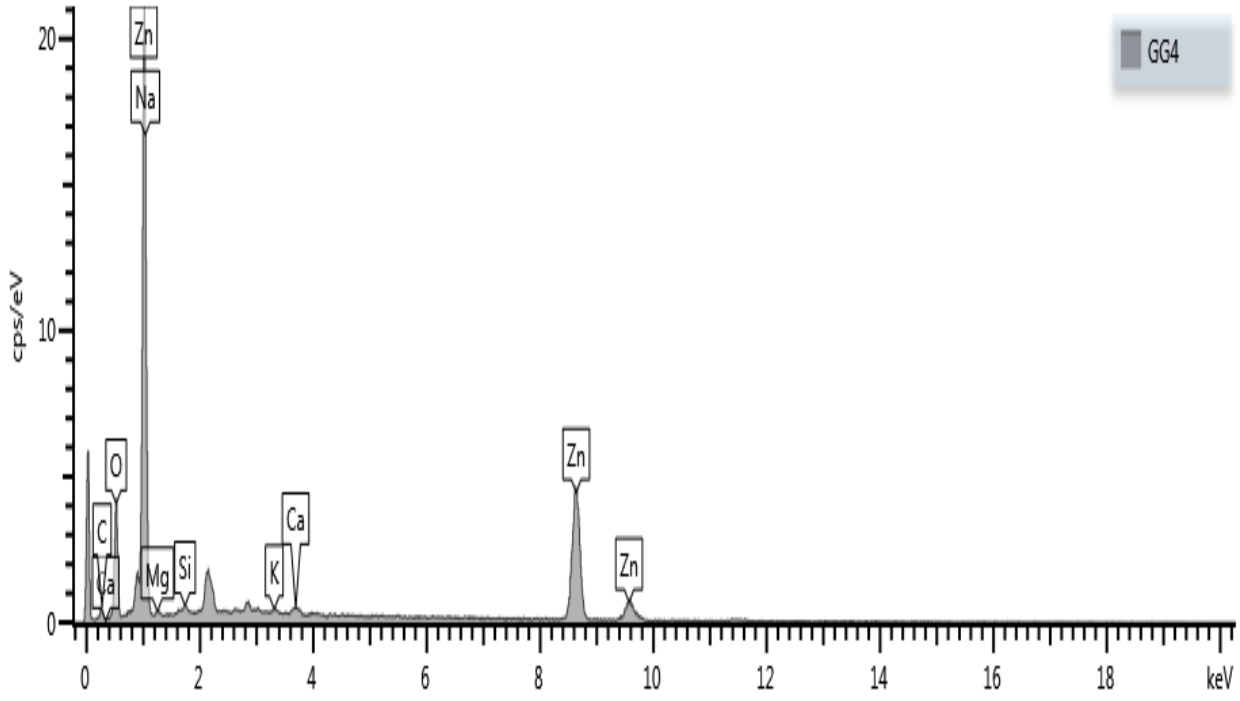

Figure 4.12: Electron Dispersive Spectrum of Optimized Bio-synthesized Zinc Oxide Nanoparticles at pH 12

4.15 X- Ray Diffraction pattern (XRD) of Optimized biosynthesized Zinc Oxide nanoparticles.

The result of X-ray diffraction patterns (XRD) of optimized biosynthesized zinc oxide nanoparticles at pH 7, 10, 12 and 12 ais presented in Figure 4.13. The intensed peak for the sample were obtained at pH7 the intense peak were at 2θ 31.77°, 34.42°, 36.25, 47.54°, 56.60°, 62.86°, 67.96° aid 69.10° corresponding this intense peaks also goes for pH 10, 11 and 12

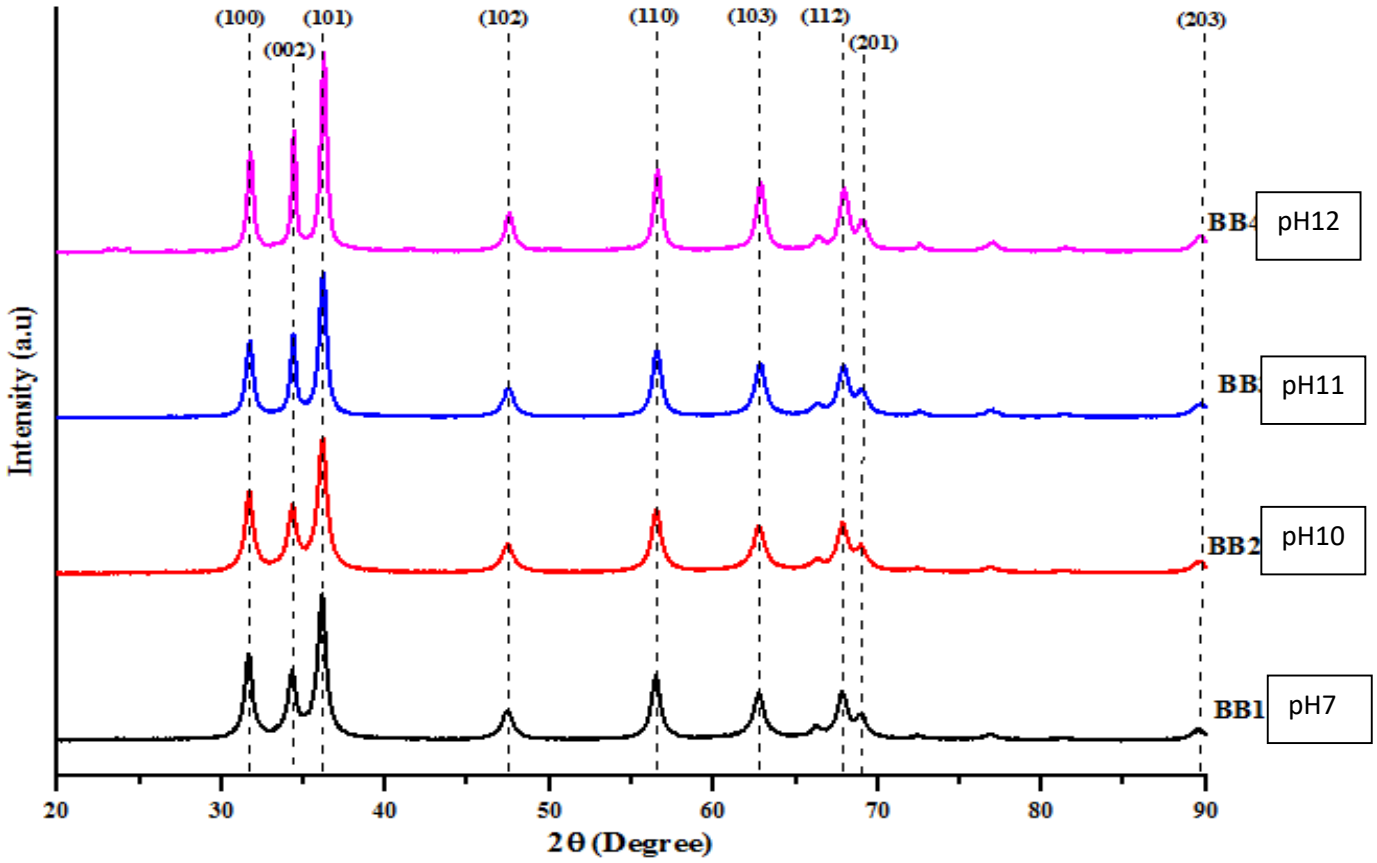

Figure 4.13: X-ray Diffraction Pattern (XRD) of Optimized Bio-synthesized Zinc Oxide Nanoparticles at pH 7, 10, 11 and 12

4.16 Fourier Transmission Infra-red Spectral of biosynthesized Zinc Oxide Nanoparticles

The result of Fourier transmission infra-red spectra (FT-IR) spectral of biosynthesized zinc oxide nanoparticle is presented in Figure 4.13. The broad peaks is in the range of 500 to 4,500 and the higher broad peaks are at 3493cm^{-1} and 2893^{o}cm^{-1}, while the lower peaks 1658 and 1469cm^{-1} other borad peaks are between 500-1450cm^{-1}

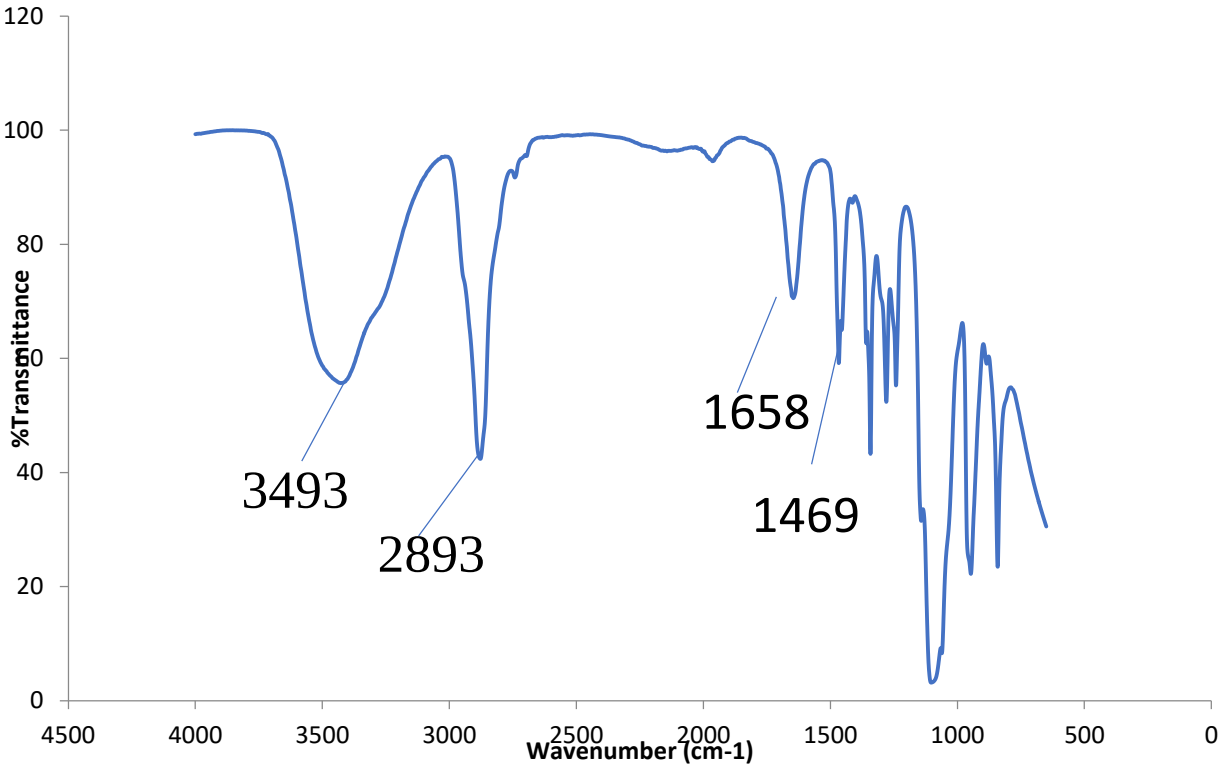

Figure 4.13: FT-IR Spectral of Biosynthesized Zinc Oxide Nanoparticle

4.17 Fourier Transmission Infra-red Spectral (FT-IR) of biosynthesized Silver Nanoparticles.

The result of Fourier transmission infra-red spectra (FT-IR) of biosynthesized silver nanoparticle is presented in Figure 4.15. The broad peak is between the range of 500-4500cm^{-1}. The higher broad peaks are at 3469cm^{-1} and 2888cm^{-1} while the lower broad peaks are at 1652cm^{-1} and 1468 cm^{-1} other are between the range of 500-1450cm^{-1}

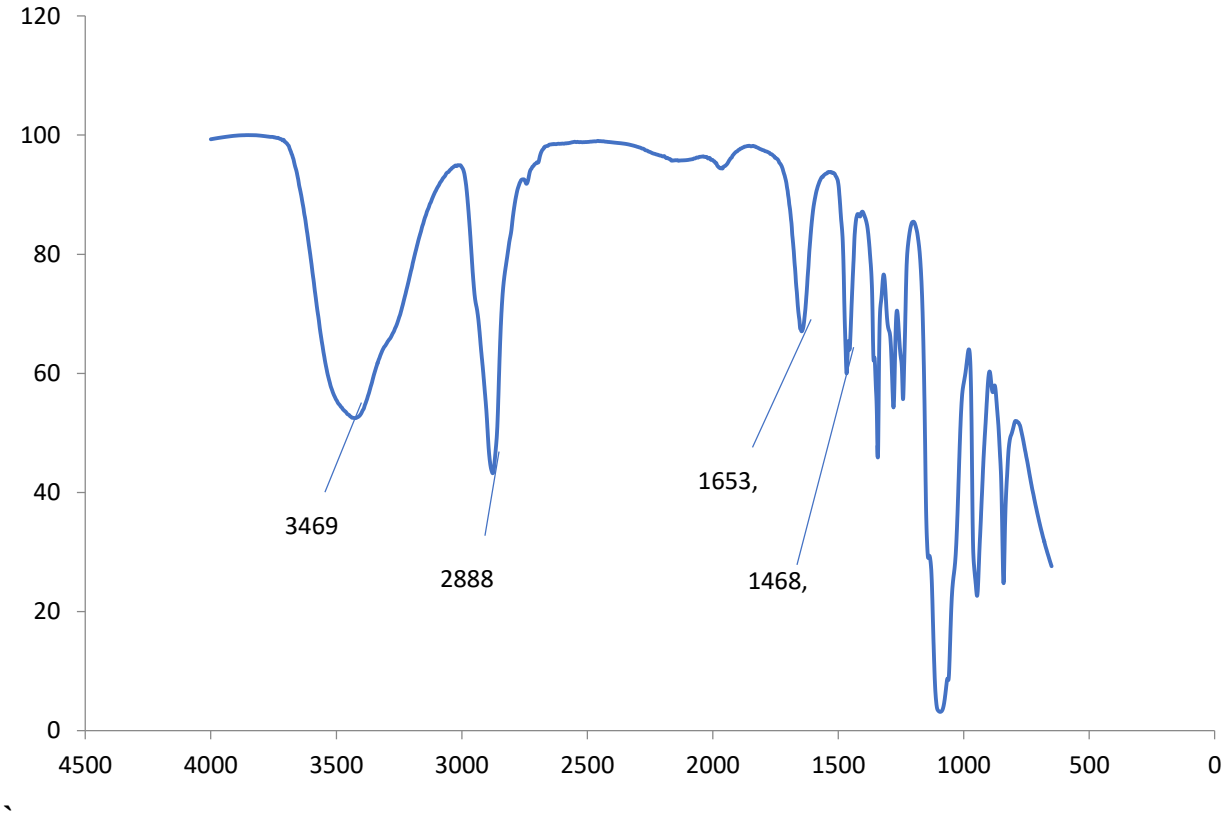

Figure 4.14: FTIR Spectra of Silver Nanoparticles Synthesized

4.18 Antimicrobial Properties of Doped and Undoped Plant-Based Synthesize Zinc Oxide and Silver

Antimicrobial Properties of Doped And Undoped Plant-Based Synthesize Zinc Oxide and Silver Nanoparticles is Presented in Table 4.2. The inhibitory activities of ZnONps against *P.aeruginosa, S.aureus* and *E. coli* revealed that the ZnONps had no zone of inhibitions. However, amoxil had inhibitory activity against *P.aeruginosa*, *S.aureus* and *E. coli* respectively. The inhibitory activities of AgNPs against *P. aeruginosa* , *E. coli, S. pyogenes* and *S. aureus* have significantly higher inhibitory activities compared to the positive standard (amoxil). The inhibitory activities of Doped ZnO/AgNPs were significantly lower in extract treated group as compared to standard and normal control.

Table 4.2. Mean Antimicrobial Susceptibility Test Result

Undoped and doped metal	ZnONps				AgNPs				Doped ZnO/AgNPs			
Concentration/ Control(mg/ml)	*P.aeruginosa*	*E. coli*	*S.pyogenes*	*S.aureus*	*P.aeruginosa*	*E. coli*	*S.pyogenes*	*S.aureus*	*P.aeruginosa*	*E.coli*	*S.pyogenes*	*S.aureus*
20	0 ± 0.0^{a}	0 ± 0.0^{a}	0 ± 0.0^{a}	0 ± 0.0^{a}	0 ± 0.0^{a}	7.5 ± 0.5^{a}	14.0 ± 1.0^{a}	15.0 ± 0.0^{a}	0 ± 0.0^{a}	8 ± 0.0^{a}	0 ± 0.0^{a}	10 ± 0.0^{ab}
40	0 ± 0.0^{a}	0 ± 0.0^{a}	11 ± 1.0^{b}	0 ± 0.0^{a}	16.5 ± 0.5^{c}	9 ± 0.0^{ab}	16.5 ± 0.5^{a}	17.5 ± 0.5^{b}	0 ± 0.0^{a}	10.5 ± 0.5^{ab}	11 ± 1.0^{b}	14 ± 1.0^{bc}
60	0 ± 0.0^{a}	0 ± 0.0^{a}	14 ± 1.0^{bc}	0 ± 0.0^{a}	17.5 ± 1.5^{c}	10.5 ± 0.5^{b}	17.5 ± 1.5^{a}	21 ± 1.0^{c}	0 ± 0.0^{a}	14 ± 3.0^{b}	14 ± 1.0^{bc}	16.5 ± 2.5^{c}
Amoxil	11.5 ± 0.5^{b}	14 ± 1.0^{b}	15 ± 1.0^{c}	21.5 ± 0.5^{b}	11.5 ± 0.5^{b}	14 ± 1.0^{c}	15.0 ± 1.0^{a}	21.5 ± 0.5^{c}	11.5 ± 0.5^{b}	14 ± 1.0^{b}	15 ± 1.0^{c}	21.5 ± 0.5^{d}
Control (Metal)	0 ± 0.0^{a}	0 ± 0.0^{a}	11 ± 1.0^{b}	0 ± 0.0^{a}	10 ± 0.0^{b}	7.5 ± 0.5^{a}	14.0 ± 0.5^{a}	15.0 ± 0.0^{ab}	0 ± 0.0^{a}	8 ± 1.0^{a}	11 ± 1.0^{b}	8 ± 0.0^{a}

Results shows zone of inhibition size mean ± standard error of mean of duplicate determination. Values with the same superscript letters in the same column are not significantly different at $p<0.05$

Key: ZnO: Zinc Oxide nanoparticles; AgNps: Silver nanoparticles

4.19 Minimum Inhibitory (MIC) and Bactericidal (MBC) Concentrations of Doped And Undoped Plant-Based Synthesize Zinc Oxide and Silver Nanoparticles

The minimum inhibitory (mic) and bactericidal (mbc) concentrations of doped and undoped plant-based synthesize zinc oxide and silver nanoparticles is presented in Table 4.3. The inhibitory activities of of Doped And Undoped Plant-Based Synthesize Zinc Oxide and Silver Nanoparticles against *E. coli, S. aureus, S, pyrogenes and P, aeruginosa* revealed that the ZnONps, AgNps and Doped ZnO/AgNps had no zone of inhibition for the MBC test. However, for the MIC, among the three extracts, ZnONps have significantly higher inhibitory activities for the four organisms tested, followed by Doped ZnO/AgNps, while AgNps have the least minimum inhibitory activity.

Table 4.3: Minimum Inhibitory (MIC) and Bactericidal (MBC) Concentrations of Doped And Undoped Plant-Based Synthesize Zinc Oxide and Silver Nanoparticles

Test Organism	MIC (mg/ml)			MBC (mg/ml)		
	ZnONps	AgNps	Doped ZnO/AgNps	ZnONps	AgNps	Doped ZnO/AgNps
E. Coli	20	5	10	I.N	I.N	I.N
S. aureus	20	5	10	I.N	I.N	I.N
S.pyrogen	10	10	10	I.N	I.N	I.N
P. aeruginosa	20	5	10	I.N	I.N	I.N

Note: I. N. = Inhibitory or Bacteriostatic;

4.2 Discussion

However, this present study, confirmed ten phytochemical constituents of the aqueous leaves extract of *Senna occidentalis* (Table 1), which is in accordance with previous work of Aja *et al.*, (2010), who also confirmed the presence of tannis, cardiac glycosides, saponins, anthraquinone and trepenoids in the aqueous leaf extract of *Senna occidentials*. The synthesis of metallic nanoparticles has been attributed to poly phenolic compounds such as Saponins and flavonoids presence in the plant extract. Previous studies have reported the synthesis of silver and zinc oxide nanoparticles using plant extract such as *Hipposphaer hamnoides, Zizip. Husoenoplia*, (L) Mill, *Hypti suaveolens, A. racemosus, S. cumini, B D Cerasifera aqueous* (Abalaka *et al.,* 2011). The extract reported rapid green synthesis of the nanoparticles due to the presence of alkaloids and flavonoids (Aja *et al.,* 2010).Therefore, the presence of alkaloids and flavonoids in *Senna occidentalis* suggested its usefullness in silver and zinc oxide nanoparticle synthesis.

Spectroscopy is the measure of the intensity of light absorbed by the nanoparticles versus the wavelength of the intensity of light ultra-violet region absorbance using spectrophotometer.This has been reported as a technique very important in characterizing nanoparticles (*Chen et al.,* 2014). The effects of ZnO nanoparticles at different pH solutions are shown in Figure 4.1 to 4.4. The spectral showed that absorption is strong at the wavelength of 329 nm for the solution pH 7, other minimal wavelength of 250, 275 and 300nm showed the ZnO nanoparticle was synthesized. Subsequently, with increasing pH 10, 11 and 12 of ZnO nanoparticle, there was similar absorbance and blue shift in the curves of wavelength, which gave a constant wavelength of 393nm for pH 10, 11 and 12. This prominent peak was as a result of band gap absorption for ZnO from the valence band to the conduction band and electron removal, this corresponds to the findings by Hashim *et*

al., (2020) who synthesized ZnO nanoparticles using *Olea europaea* leaf extract and confirmed UV-visible spectral with a peak at 370 nm for varying pH of 7, 10, 11, 12, 14 and 18 and observed a blue shift in the curves of wavelength. The characteristic broad peak of ZnO nanoparticles have absorption in UV region ranging between 210-400 nm. The size of synthesized ZnO nanoparticles using DLS as presented in Figure 4.5 as the mean size of 52.50 nm and polydispersity index (PDI) of 0.731, which is closed to the value obtained by Gupta *et al.* (2018). The PDI shows that the synthesized nanoparticles are monodispersed.

Figure 4.6 shows the UV wavelength of synthesized Ag nanoparticles and the *Senna occidentalis* extract at pH 7. *Senna occidentalis* extract added to $AgNO_3$ gave a change in colour from a white to dark brown. This corroborate with the already reported finding in which similar colour turned into dark brown which indicate the formation of silver nanoparticles (Hashim *et al.,* 2020). This was as a result of excitation of surface plasmon resonance in the metal nanoparticles which occurred due to the combination of metal nanoparticles electron vibration with the light wave. The characteristics board peak of Ag nanoparticles normally appears at a wavelength interval of 300 – 600 nm Vasireddy *et al.,* (2012). The size of synthesized Ag nanoparticles using DLS as shown in Figure 4.7 as the mean size of 83.40 nm. The Ag nanoparticles in aqueous solution of the silver complex was reduced using the extract of *Senna occidentalis* under UV visible spectral. The peaks between 270 and 334.5 nm were for *Senna occidentalis* while the combination of the extract with Ag salt solution had 267.5 and 331 nm (Figure 4.6). Peaks become broad and not sharp in the combined extract and Ag salt solution and there was a slight shift in wavelength when compared to the extract alone. This may be due to the size distribution of the particles and a complete reaction of the silver ions that took place at a faster rate.

Transmission electron microscopy (TEM) is a microscopy technique in which a beam of electrons is transmitted through nanoparticles, interacting with the nanoparticles as it passes through with an image formed from the interaction of the electron transmitted through the nanoparticles (Shobba *et al.,* 2014). The morphology, size and crystalline nature of the Ag nanoparticles using HRTEM, and SAED analysis were employed.

The HRTEM(High Resolution Thermal Electron Microscope) image of the synthesized Ag nanoparticles indicates that the synthesized nanoparticles are spherical and agglomerated in shape as shown in Plate II(A). The uniform lattice fringes as shown in Plate(B) shows that the spherical particles are crystallized, having lattice spacing of 0.23 nm which correspond to (111) planes of Ag. The SAED (Selected Area Electron Diffraction) pattern of biosynthesized silver nanoparticles showed in Plate III has a symmetry diffraction spots which confirmed that the spherical nanoparticles are crystalline and indexed to (111) plane of Silver. The synthesized Ag nanoparticles size of 8.04 nm was determined using image J software. The size of Ag nanoparticles is similar with findings of Abdel-Raouf *et al.,* (2018) who used *Padina Pavoma aqueous* extract in production of Ag nanoparticle and observed a diversed size of 8.05 nm. Furthermore, the variation in the size of Ag nanoparticles could be attributed to the existence of polyphenolic compounds from *Senna occidentalis* that have strong intermolecular forces between the extract and Ag salt solution.

The HRTEM pattern of biosynthesized ZnO nanoparticles is shown in Plate III. The HRTEM (A) image of the synthesized ZnO confirmed that the particles are hexagonal with the average particle size to be 20 nm. This finding correspond to the finding of Pavithra *et al.,* (year) who synthesized ZnO nanoparticles using aqueous leaf extract of *Tabernaemontana divaricata* green leaf extract whose particles were hexagonal with

particle size ranging from 20nm. The SAED pattern plate V of the biosynthesized ZnO showed that the diffraction rings have sharp spot revealing polycrystalline nature with symmetrical orientation of ZnO nanoparticles. The HRTEM microscopy pattern is indexed (010), (002) and (101) planes and the crystallinity of the ZnO nanoparticles has the lattice fringes of 2 nm which correspond to (101) plane of ZnO.

Electron dispersive xray (EDX) is a technique used for elemental analysis which is based on the generation of characteristics Xrays in atoms of the nanoparticles by the incident beam electrons, (Samuelson *et al.*, 1998). EDX techniques is used in the study of drugs delivery in order to detect nanoparticles that is generally used to improve the therapeutic performance of chemotherapeutic agents.

The elemental analysis of optimized Ag nanoparticles was analyzed using EDX spectroscopy. Figure 4.10 shows EDX spectrum of Ag nanoparticles with observed peaks corresponding to the binding energies of Ag nanoparticles. The peaks with the binding energies of 0.82, 1.1, 8.03 and 8.93 keV correspond to Copper(Cu) . the peak located at 0.25 keV is related to Carbon(C) as observed in Figure 4.10. The presence of Cu and C peaks are due to carbon coated copper grid of TEM. The EDX profile of the sample showed that the Ag nanoparticles contain silver, with no oxide and other impurities detected.

The EDX analysis was investigated to know the elemental composition of the biosynthesized ZnO nanoparticles. The EDX spectrum of ZnO nanoparticle prepared at different pH values are displayed in Figure 4.11 to 4.4.14. The nanoparticles are mainly composed of Zinc and Oxygen. The peaks of Zinc (Zn) are situated at the binding energies of 1.0, 8.8 and 9.8 keV. The presence of calcium (Ca) could be attributed to plant extract used during biosynthesis of ZnO nanoparticles, Sodium (Na) is from the precipitating agent and carbon (C) is from the carbon supported film on the grid.

The phase and crystallite size of the synthesized ZnO nanoparticles at pH of 7, 10, 11 and 12 were determined by XRD pattern as shown in Figure 4.15, this corroborated with the findings of Ghamsari *et al.*, (2014) whose results revealed the formation of nanocrystalline phase of ZnO nanoparticles with intense peaks for the sample at $2\theta = 31, 35, 37, 47, 56, 63, 67, 68, 70$ which corresponded to lattice plane (100) , (002), (101), (102), (110), (103), (200), (112), (201).

All the ZnO samples with diffraction line (101), (002) and (101) are sharper than other diffraction lines as seen in Fig. 4.15. It was observed that as the pH became more basic, the diffraction lines were broadened, causing particles to become smaller. This formation resulted to smaller nanoparticles at high pH. The average crystallite size of 12.03, 10.21, 9.18 and 8.07 nm of biosynthesized ZnO nanoparticles at pH 7, 10, 11 and 12, respectively. The results matched with the report of Chaudhuri and Malodia (2017) on the biosynthesis of ZnO nanoparticles using the leaf extract of *Calotropis gigantean*.

Fourier Transform Infared (FTIR) spectroscopy measures infra-red intensity versus wavelength of light. It is used to determine the nature of associated functional groups and structural features of biological compounds with nanoparticles (Amudha *et al*., 2014).

Figure 4.16 depicted the FTIR spectrum of the optimized ZnO nanoparticles in the range of 500 to 4500 cm^{-1}. The broad peak at 3493 cm^{-1} correspond to OH group stretching. This peak related to hydrogen bond is due to air humidity. The band peak appeared at 11658 cm^{-1} is assigned to –COO– band while 1469 cm^{-1} corresponds to symmetric C=O vibrations. The presence of C=O in FTIR spectra could be as a result of zinc salt precursor. The absorption bands observed at 530 to 720 cm^{-1} correspond to ZnO bonding, which result from the formation of covalent bond between zinc metal and oxygen atom. A similar findings was observed by Efafi *et al.,* (2014) and Sundra Rajai *et al.*, (2015) who reported

FTIR spectrum of biosynthesized ZnO nanoparticles to exhibit several peaks at 3429 (O-H), 1527 – 1670 (N-H) and 1076 (C-O) or 880 – 1380 (RCOO) cm^{-1}.

The FTIR spectra of biosynthesized Ag nanoparticles showed peaks at 3490, 2888, 1653, 1468, 1190, 930 and 743 cm^{-1} as present in Figure 4.17. The broad absorption peak of Ag nanoparticles at 3469 cm^{-1} relates to OH stretch of phenolic group, the peak at 1640cm^{-1} (C=0, C=N, and C=C) is correspond to amide I and amide II linkages of protein while peak 3300cm^{-1} is responsible for binding vibrations of N-H groups. The sharp peak at 2888 cm^{-1} corresponds to asymmetric –CH stretching of $–CH_2$ group and –CN group of amines. The peak shown at 1653 cm^{-1} and 1468 cm^{-1} are related to C=O and C=C bending mode of vibrations. The peak at 1190 cm^{-1} is attributed to C-O stretching of phenolic compounds present in the leaf extract of *Senna occidentalis* which binds with the surface of Ag, thus leading to the stabilization of the synthesized nanoparticles. The spectrum of Ag nanoparticles correspond to the peak at 842 cm^{-1} which could bind with the protein molecule of plant extract, this findings corresponds with the work of Hassan *et al.,* (2019), whose FTIR results for Ag nanoparticles showed maximum bands at 1640 and 3300.

The results of antimicrobial susceptibility test of doped and undoped plant-based synthesize zincoxide and silver nanoparticles tested against standardized inoculum of *P. aeruginosa*, *E. coli, S. pyogenes* and *S. aureus* using various concentrations of the extract at 20 mg/ml, 40 mg/ml and 60 mg/ml are bening express in Table 4.1. The doped and undoped plant-based synthesized nanoparticles tested, exhibited antibacterial activity on almost all the selected bacteria pathogens at various degree. Undoped zinc oxide nanoparticle (ZnNPs) showed activity only against *S. pyogenes* to be 11-14 mm while against *P. aeruginosa*, *E. coli* and *S. aureus* were found to be resistant (Table 4.1). For the silver nanoparticle (AgNPs) it was found to have antibacterial activity against *P. aeruginosa*, *E. coli, S.*

pyogenes and *S. aureus* to be 16-17mm, 7.5-10 mm, 14-17 mm and 15-21 mm respectively (Table 4.1). *E. coli, S. pyogenes* and *S. aureus* were found to be susceptible to doped zinc oxide and silver nanoparticles (Zn/AgNPs) with the following zones of inhibitions 8-14 mm, 11-14 mm and 10-16 mm while *P. aeruginosa* was not susceptible to it as expressed in Table 4.1. For the positive control amoxil antibiotics was used which gave the following zone of inhibition 11 mm, 14 mm, 15 mm and 21 mm for *P. aeruginosa*, *E. coli*, *S. pyogenes* and *S. aureus* respectively (Table 4.1). The metals that was used to synthesized the nanoparticles which include zinc oxide, silver trioxonitrite and doped zinc oxide/trioxonitrite as negative control. For zincoxide, recorded 11mm against *S. pyogenes* and resistant to *P. aeruginosa*, *E. coli* and *S. aureus.* From Table 4.1, it was revealed that the following zones of inhibitions were obtained 10 mm, 9.5 mm, 14 mm and 7.5 mm against *P. aeruginosa, E. coli, S. pyogenes* and *S. aureus* respectively. Doped Zn/AgNPs had no activity on *P. aeruginosa* while *E. coli, S. pyogenes* and *S. aureus* showed activity to be 8 mm, 11 mm and 8 mm respectively.

It was found that doped and undoped plant-based synthesize zinc oxide and silver nanoparticles had antimicrobial properties at varying degree when the concentration of the extract was tested against some selected pathogens. Upon increasing the concentration of the extracts resulted increase in diameter zone of inhibition with the exception of the ZnNPs being resistant to *P. aeruginosa*, *E. coli* and *S. aureus.* This agrees with the work of Olonifade *et al.,* (2018). The rate at which antimicrobial agent inhibit the growth of bacteria is concentration dependent (Abalaka *et al.,* 2010). According to Ochei and Kolhatkat (2010), the diameter of zone of inhibition is dependent on the population of the bacteria

inoculated, the rate at which the bacteria grows and rate at which the antimicrobial agent diffused through the medium and subsequent caused damaged to the bacteria.

From this study, it was found out that AgNPs had more antimicrobial activity followed by the doped Zn/AgNPs and ZnNPs. This is not in agreement with the previous work of Ezealisiji and Xavier (2020) that reported, the doped or combined ZnNPs with mucin which gave the highest antibacterial activity. This difference could be due to method of synthesizing the NPs, the laboratory procedure for testing the NPs antibacterial activity or the strain of the bacteria pathogens. The Zinc oxide NPs displayed good antibacterial activity against *P. aeruginosa* tested in this study, as indicated by the diameter of inhibition zone. A similar result was reported in the work of Monika *et al.,* (2018), the worked on the effective antimicrobial activity of green ZnNPS of *Cathanthus roseus.* AgNPs had the highest antibacterial activity on *S. aureus,* this have been reported in the previous work of Monika *et al.,* (2018) and Carmen *et al.,* (2012)**.** In this study, results showed that AgNPs and Zn/AgNPs may have undergoes an interaction with the bacterial cell. The results indicated better action against gram-positive bacteria as compared to gram-negative bacteria, this agrees with the findings of Faizan *et al.,* (2019). The enhanced antibacterial activity of AgNPs compared to $AgNO_3$ solution is attributed to their large surface area that provides more surface contact with microorganisms. Another important reason of enhanced antibacterial activity of AgNPs as documented in the literature is the synergistic effect between particles and natural compounds (Muhammad *et al.,* 2017). The mechanism of action of the antibacterial activity of AgNPs is attacking the respiratory chain and cell division that ultimately leads to cell death one hypothesis from the research states that the silver nanoparticles invade the bacterial cell and bind to the vital enzymes containing thiol

groups (Ram and Vyshnava, 2013). The silver nanoparticles have also been reported to release silver ions inside the bacterial cells, further enhancing their bactericidal activity. It was recorded, that amoxil the positive control gave a bigger diameter zone of inhibition than the NPs s. This might be due to the fact that amoxilicilin had been properly refined and purified. There is a high chance that, when purified this doped and undoped plant-based synthesized Zn and Ag nanoparticles can perform better. Therefore, these NPs contain active antimicrobial agent as earlier reported by Macro *et al.*, (2020). Although, MBC revealed inhibitory or bacteriostatic effects of the nanoparticles, AgNps, Doped ZnONps revealed lesser values in MIC in otherwords they are more potent than the ZnONps with higher values.

CHAPTER FIVE

5.0 CONCLUSION AND RECOMMENDATIONS

5.1 Conclusion

The ZnO and Ag nanoparticles were synthesized using green synthesis method and characterized by UV visible, XRD, HRTEM, HRSEM, EDX and FTIR. The synthesis, characterization and antimicrobial properties of ZnO and Ag nanoparticles were studied. Based on these studies, the following conclusion were drawn:

The qualitative phytochemical constituents of *Senna occidentalis*is aqueous extracts include alkaloids, flavonoids, tannins, anthraquinones, phenols, terpenoids, glycosides, saponins, steroids, and phlobatanins

The peak of ZnO nanoparticles have absorption in UV region between 210-400 nm and Ag nanoparticles were between 267.5 and 331 nm

The HRTEM image of the synthesized Ag nanoparticles show that nanoparticles have spherical shapeed and not agglomerated. The HRTEM image of the synthesized ZnO confirmed that the particles are hexagonal with the average particle size to be 25-60 nm

EDX spectrum of Ag nanoparticles with detected peaks between 3.0 and 3.6 keVm while ZnO nanoparticles are mainly composed of Zn and O with the peaks of Zn situated at the binding energies of 1.0, 8.8 and 9.8 keV

The antimicrobial activity of zinc and silver nanoparticles produced inhibition of *S. pyogenes, E.coli, S. auerus* and *P aeruginosa*,

The activity of doped zinc and silver nanoparticles produced inhibition of *S. pyogenes* only amongst the tested organisms, however, the doped zinc and silver nanoparticles were not active against *E.coli, S. auerus* and *P. aeruginosa*, respectively.

5.2 Recommendation

Further studies should explore more physiologically relevant modes of bacterial interaction with nanoparticles. To better understand the capability of these nanoparticles, further studies should be carried out to know the clinical potentialss of antimicrobial nanoparticles.

REFERENCES

Abalaka M. E., Adeyemo S.O., and Daniyan S.Y. (2011). Evaluation of the Antimicrobial Potentials of Leaf Extracts of *Khaya senegalensis*, *Journal of Pharmaceutical Research and Opinion,* 1(2), 48-51.

Abdellah, N. H., & Abouelmagd, S. A. (2017). Surface functionalization of polymeric nanoparticles for tumor drug delivery: approaches and challenges. *Expert Opinion on Drug Delivery*, *14*(2), 201-214.

Abdel-Raouf, N., Al-Enazi, N.M., Ibraheem, I.B.M., Alharbi, R.M., and Aikhulaifi, M.M. (2018). Biosynthesis of Silver nanoparticles by use of the marine brown alga *Patina Povonia* and their characterization. *Saudi Journal of Biological Science,* 4(6), 54-61.

Aboada, C., Biodun, F., Gunle, T., and Dele, G. (2006). Antimicrobial activities of *Calotropis procera Journal of Ethnopharmacology*, 45, 13-17.

Abou El-Nour, K. M., Eftaiha, A. A., Al-Warthan, A., & Ammar, R. A. (2010). Synthesis and applications of silver nanoparticles. *Arabian Journal of Chemistry*, *3*(3), 135-140.

Abouelmagd, S. A., Meng, F., Kim, B. K., Hyun, H., & Yeo, Y. (2016). Tannic acid-mediated surface functionalization of polymeric nanoparticles. *ACS Biomaterials Science & Engineering*, *2*(12), 2294-2303.

Africa Center for Disease Control (2018). Africa Center for Disease Control framework for Antimicrobial resistance, 3(5), 2018- 2023.

Agarwal, N., & Brem, A. (2017). Frugal innovation-past, present, and future. *IEEE Engineering Management Review*, *45*(3), 37-41.

Ahmed, S., & Ikram, S. (2016). Biosynthesis of gold nanoparticles: a green approach. *Journal of photochemistry and photobiology Biology*, *161*, 141.

Aja P.M, Okaka ANC, Onu P.N, Ibiam U, Urako A.J, (2010). Phytochemical composition of *Talinum triangulare* (waterleaf) leaves. *Pakistan Journal of Nutrition*, 9(6), 527-530

Ajiv, P. & Rajeshwari, S. (2013). Venckatesh Bio-fabrication of zinc oxide nanoparticles using leaf extract if far *thenium hysterophorus* L. and its size is dependent on antifugal actitivity against plant fungal pathogens. Spectrochim Acta Part A. *Molecular Biomolecule Spectroscope*, 112, 384 - 387.

Akhavan, O., Azimirad, R., Safa, S., & Hasani, E. (2011). CuO/Cu (OH) 2 hierarchical nanostructures as bactericidal photocatalysts. *Journal of Materials Chemistry*, *21*(26), 9634-9640.

Al-Asady, Z. M., AL-Hamdani, A. H., & Hussein, M. A. (2020). Study the optical and morphology properties of zinc oxide nanoparticles. *International Conference on Materials Engineering & Science*, 6(7), 99-111.

Ali, A., Zafar, H., & Zia, M., ul Haq, I., Phull, A.R., Ali, J.S. (2016). Synthesis, characterization, applications, and challenges of iron oxide nanoparticles. *Nanotechnology Science and Application*, *9*, 49-67.

Ali, S., Khan, I., Khan, S. A., Sohail, M., Ahmed, R., ur Rehman, A., & Morsy, M. A. (2017). Electrocatalytic performance of Ni@ Pt core–shell nanoparticles supported on carbon nanotubes for methanol oxidation reaction. *Journal of Electroanalytical Chemistry*, *795*, 17-25.25.

American Society for Microbiology, Washington, DC. 5th Edition, 1105-1125.

Ananias, D., Paz, F. A. A., Carlos, L. D., & Rocha, J. (2013). Chiral microporous rare-earth silico-germanates: Synthesis, structure and photoluminescence properties. *Microporous and mesoporous materials*, *166*, 50-58.

Anisa, A. (2017). Meningkatkan keterampilan berpikir kritis peserta didik melalui pembelajaran IPA berbasis potensi lokal Jepara. *Jurnal Inovasi Pendidikan IPA*, *3*(1), 1-11.

Anisa, N. (2003). Analisis Faktor-Faktor Yang Mempengaruhi Return Saham (Studi Kasus Pada Perusahaan Sub Sektor Automotive And Components Yang Terdaftar Di Bursa Efek Indonesia Periode 2010-2014). *Perbanas Review*, *1*(01), 34-49.

Ankanna, S. Prasad, T.N.V.K.V., Elumalai, E.K., & Savithramma, N. (2010). Production of biogenic silver nanoparticles using *Boswellicius Valifoliolata* stem bark. Dig *Journal of Nano material Biostructure*, 5, 369-372.

Aqel, A., Abou El-Nour, K. M., Ammar, R. A., & Al-Warthan, A. (2012). Carbon nanotubes, science and technology part (I) structure, synthesis and characterisation. *Arabian Journal of Chemistry*, *5*(1), 1-23.

AshaRani, P. V. (2009). Low Kah Mun G, Hande MP, Valiyaveettil S. Cytotoxicity and genotoxicity of silver nanoparticles in human cells. *ACS Nano*, *3*(2), 279-290.

Azizi, S., Ahmad, M. B., Namvar, F., & Mohamad, R. (2014). Green biosynthesis and characterization of zinc oxide nanoparticles using brown marine macroalga Sargassum muticum aqueous extract. *Materials Letters*, *116*, 275-277.

Binns, C. (2010). Introduction to Nanoscience And Nanotechnology. *Biointerfaces*, *73*(1), 51-57.

Bu, Y., Wang, S., Jin, H., Zhang, W., Lin, J., & Wang, J. (2012). Synthesis of porous NiO/reduced graphene oxide composites for supercapacitors. *Journal of the Electrochemical Society*, *159*(7), A990.

Buffat, P., & Borel, J. P. (1976). Size effect on the melting temperature of gold particles. *Physical Review*, *13*(6), 2287.

Carmen, S. C., Simona, L. I., Ariana, C. C., Adrian, C., Philippe, L., & Daniela. P. (2012) Synthesis and Antimicrobial Activity of Silver-Doped Hydroxyapatite Nanoparticles, *Biomed Research International*, (6), 10-20.

Chanda, S., Kaneria, M., & Vaghasiya, Y. (2001). Evaluation of antimicrobial potential of some indian medicinal plant against some pathogenic microbes. *Indian Journal National Production Reserve*, 2, 225-228

Chang, C. W., Wu, H. T., Huang, S. H., Chen, C. K., Un, I. W., & Yen, T. J. (2013). Singlecrystalline heterostructure of ZnO nanowire arrays on large Ag microplates and its photocatalytic activity. *Acta materialia*, *61*(18), 6993-6999.

Chao, W., Dennis, V., Karren, L., More, Nestor, J., Zaluzec, S., shouheng, S., hideo, D., Guofeng, W., & Jeffrey, G. (2011). Multimetallic Au/Fe pt3 Nanoparticles as highly durable Electrocatalyst. *Nano Letters*, 11(3), 919-926.

Chaudhuri, S. K., & Malodia, L. (2017). Biosynthesis of zinc oxide nanoparticles using leaf extract of Calotropis gigantea: characterization and its evaluation on tree seedling growth in nursery stage. *Applied Nanoscience,* 7(8), 501–512.

Chen, C., Trindade, F. Z., de Jager, N., Kleverlaan, C. J., & Feilzer, A. J. (2014). The fracture resistance of a CAD/CAM Resin Nano Ceramic (RNC) and a CAD ceramic at different thicknesses. *Dental Materials*, *30*(9), 954-962.

Chen, Q., Jiang, H., Ye, H., Li, J., & Huang, J. (2014). Preparation, antibacterial, and antioxidant activities of silver/chitosan composites. *Journal of Carbohydrate Chemistry*, *33*(6), 298312.

Chen, Y. L., & Li, Q. Z. (2007). Prediction of apoptosis protein subcellular location using improved hybrid approach and pseudo-amino acid composition. *Journal of Theoretical Biology*, *248*(2), 377-381.

Chien, C. H., Chiou, S. H., Guo, G. Y., & Yao, Y. D. (2004). Electronic structure and magnetic moments of 3d transition metal-doped ZnO. *Journal of Magnetism And Magnetic Materials*, *282*, 275-278.

Cho, J., & Lee, S., (2004). Comparison of ceramic and polymeric membranes for natural organic matter (NOM) removal. *Desalination*, *160*(3), 223-232.

Chou, S.Y., Grossman, M., & Saffer, H. (2004). An economic analysis of adult obesity: result from the behaviour risk factor surveillance system. *Journal of Health Economics*, 23,565-587.

Clark Jr, L. C., & Lyons, C. (1962). Electrode systems for continuous monitoring in cardiovascular surgery. *Annals of the New York Academy of sciences*, *102*(1), 29-45.

Clark L.C., & Lyons. C. (1962). Electrode systems for continuous monitoring in cardiovascular surgery. *Ann New York Academy Science,* 102(1), 29 - 45.

Coyle, M.B. (2005). Manual of antimicrobial Susceptibility testing, *American Society for Microbiology* , 6(7), 77-84.CU nanoparticle accumulation of copper in the Isopod *Porce U10 Scaber* is due to the dissolved CU ions inside the digestive ract. *Environment Science Technology*, 46, 12112 - 12119.

Danelon, M., Pessan, J. P., Neto, F. N. S., de Camargo, E. R., & Delbem, A. C. B. (2015). Effect of toothpaste with nano-sized trimetaphosphate on dental caries: In situ study. *Journal of Dentistry*, *43*(7), 806-813.

Deepak, V., Umamaheshwaran, P. S., Guhan, K., Nanthini, R. A., Krithiga, B., Jaithoon, N. M. H., & Gurunathan, S. (2011). Synthesis of gold and silver nanoparticles using purified URAK. *Colloids and Surfaces Biointerfaces*, *86*(2), 353-358.

Dong, H., Wen, B., & Melnik, R. (2014). Relative importance of grain boundaries and size effects in thermal conductivity of nanocrystalline materials. *Scientific reports*, *4*(1), 1-5.

Dong, X., Chen, J., Ma, Y., Wang, J., Chan-Park, M. B., Liu, X., & Chen, P. (2012). Superhydrophobic and superoleophilic hybrid foam of graphene and carbon nanotube for selective removal of oils or organic solvents from the surface of water. *Chemical Communications*, *48*(86), 10660-10662.

Dreaden, E. C., Alkilany, A. M., Huang, X., Murphy, C. J., & El-Sayed, M. A. (2012). The golden age: gold nanoparticles for biomedicine. *Chemical Society Reviews*, *41*(7), 27402779.

Duan, X., & Li, Y. (2013). Physicochemical characteristics of nanoparticles affect circulation, biodistribution, cellular internalization, and trafficking. *Nanoscience, 9*(10), 1521-1532.

Durán, N., Marcato, P. D., De Souza, G. I., Alves, O. L., & Esposito, E. (2007). Antibacterial effect of silver nanoparticles produced by fungal process on textile fabrics and their effluent treatment. *Journal of Biomedical Nanotechnology*, *3*(2), 203-208.

Ebadifar, A., Nomani, M., & Fatemi, S. A. (2017). Effect of nano-hydroxyapatite toothpaste on microhardness ofartificial carious lesions created on extracted teeth. *Journal of Dental Research, Dental Clinics, Dental Prospects*, *11*(1), 14.

Ezealisiji, K. M. and Xavier, S. (2020) Green Synthesis of Zinc Oxide Nanoparticles and Their Antibiotic-potentiation Activities of Mucin Against Pathogenic Bacteria. *Research Journal of Nanoscience and Nanotechnology,* 10(3923),1996-5044.

Faizan, A., Anam, S., Haris, M. K., Fohad, M. H., Rais, A. K., Bader, A., Ali A., and Iqbal, A. (2019). Antibacterial Effect of Silver Nanoparticles Synthesized Using *Murraya koenigii* (L.) against Multidrug-Resistant Pathogens, *Bioinorganic Chemistry and Applications,* 46(49) 50-61.

Fateh, R., Dillert, R., & Bahnemann, D. (2014). Self-cleaning properties, mechanical stability, and adhesion strength of transparent photocatalytic TiO2–ZnO coatings on polycarbonate. *ACS Applied Materials & Interfaces*, *6*(4), 2270-2278.

Fowsiya, J., Madhumitha, G., Al-Dhabi, N. A., & Arasu, M. V. (2016). Photocatalytic degradation of Congo red using Carissa edulis extract capped zinc oxide nanoparticles. *Journal of Photochemistry and Photobiology*, *162*, 395-401.

Franci, G., Falanga, A., Galdiero, S., Palomba, L., Rai, M., Morelli, G., & Galdiero, M. (2015). Silver nanoparticles as potential antibacterial agents. *Molecules*, *20*(5), 8856-8874.

Gad, M., ArRejaie, A. S., Abdel-Halim, M. S., & Rahoma, A. (2016). The reinforcement effect of nano-zirconia on the transverse strength of repaired acrylic denture base. *International Journal of Dentistry, 3(4),* 56-63.

Gamanni, G., Roche, V., Childs, C., Mazo, M., and Ackermann, R.V. (2015).The three dimensional geometry of relay zones within segmented normal faults. *Journals of structural geometry*, 129, 10-18.

Getie, A., Belay, A. R., Chanda, R., and Belay, D. (2017). Synthesis and Characterization of zinc oxide nanoparticles for Antibacteria Applications, *Journal of Nanomedicine and Nanotechnology,* 8(9), 2157 – 2524.

Ghamsari, M.S., Alamdari, S; Razzaghi D;, Pirlar, M.A; ZnO nanocrystals with narrow-band blue emission. *Journal of Lamination,* 2019, 205 - 508 - 518.

Gopal, P., & Spaldin, N. A. (2006). Magnetic interactions in transition-metal-doped ZnO: An ab initio study. *Physical Review, 74*(9), 094418.

Govanni, G., Zavattero, E., Stefano, V., Ramieri, G., & Gerbino, G. (2015). Treatment of orbital mesh wall fractures with titanium mesh plates using retrocaruncular approach: outcomes with different techniques. *Hindawi,* 5(6), 76-83.

Gupta, M., Tomar, R. S., Kaushik, S., Mishra, R. K., & Sharma, D. (2018). Effective antimicrobial activity of green ZnO nano particles of Catharanthus roseus. *Frontiers in microbiology*, *9*, 20, 30.

Gurunathan, S. (2015). Biologically synthesized silver nanoparticles enhances antibiotic activity against Gram-negative bacteria. *Journal of Industrial and Engineering Chemistry*, *29*, 77-84.

Harbone, J.b. (1973). Phytochemical methods. In Harbone J.B (ed) A guide to modern techniques of plant analysis. Chapman and Hall, London. 67.

Hasanzadeh, M., & Shadjou, N. (2016). Electrochemical nanobiosensing in whole blood: Recent advances. *TrAC Trends in Analytical Chemistry*, *80*, 167-176.

Hashim, N., Paramasivam, M., Tan, J.S., Kernain, D., Hussin, M.H., Brosse, N., Gambier, F. and Raja, P.B. (2020). Green mode synthesis of silver nanoparticles using Vitis vinifera's tannin and screening its antimicrobial activity/apoptotic potential versus cancer cells. *Materials Today Communications*, *25*, 10-16.

Hassan, S.E.D., Suem, S.S., Fouda, A., Awwad, M.A., Awad, I., Gana, M.S., Abdu, M.A. (2018). New Approach for antimicrobial activity and bio-control of various pathogens by biosynthesized and copper nanoparticles using endophyticactinomyces. *Journal Radiation Reserve. Application of Science*, 11, 262 - 270.

Hisatomi, T., Kubota, J., & Domen, K. (2014). Recent advances in semiconductors for photocatalytic and photoelectrochemical water splitting. *Chemical Society Reviews*, *43*(22), 7520-7535.

Holzinger, M., Le Goff, A., & Cosnier, S. (2014). Nanomaterials for biosensing applications: a review. *Frontiers in Chemistry*, *2*, 63.

Hussein, M.F., Sadek, O.A., & El Taher, S.G. (2015). Occurrence of Bacillus cereus and staphylococcus aureus organisms in some dairy desserts. Assiut veteinary medicine Hournal. 61 (145), 160-165.

Igbinosa, O.O., Igbinosa E.O., and Aiyegoro, O.A. (2009). Antimicrobial activity and phytochemical screening of stem bark extracts from *Jatropha curcas* (Linn.), *African Journal of Pharmacy and Pharmacology*, 3(2), 58-62.

Iravani, S. (2014). Green Synthesis of metal nanoparticles using plants. *Green Chemistry*, 13, 2638 - 2650.

Ivanisevic, I. (2010). Physical stability studies of miscible amorphous solid dispersions. *Journal of Pharmaceutical Sciences*, 99(9), 4005-4012.

Jeevan, P., Ramya, K., & Rena, A.E. (2012). Extracellular biosynthesis of silver nanoparticles by culture supernatant of *pseudomonas aeruginosa. Indian Journal Biotechnology*, 11, 72 - 76.

Jo, D. H., Kim, J. H., Lee, T. G., & Kim, J. H. (2015). Size, surface charge, and shape determine therapeutic effects of nanoparticles on brain and retinal diseases. *Nanomedicine: Nanotechnology, Biology and Medicine*, 11(7), 1603-1611.

Kalimuthu, K., Babu, R. S., Venkataraman, D., Bilal, M., & Gurunathan, S. (2008). Biosynthesis of silver nanocrystals by Bacillus licheniformis. *Colloids and surfaces Biointerfaces*, *65*(1), 150-153.

Kalishwaralal, K., Banumathi, E., Pandian, S. R. K., Deepak, V., Muniyandi, J., Eom, S. H., & Gurunathan, S. (2009). Silver nanoparticles inhibit VEGF induced cell proliferation and migration in bovine retinal endothelial cells. *Colloids and Surfaces Biological*, 32(5), 43-55.

Kalishwaralal, K., BarathManiKanth, S., Pandian, S. R. K., Deepak, V., & Gurunathan, S. (2010). Silver nanoparticles impede the biofilm formation by Pseudomonas aeruginosa and Staphylococcus epidermidis. *Colloids and Surfaces Biointerfaces*, *79*(2), 340-344.

Kalishwaralal, K., Deepak, V., Pandian, S. R. K., Kottaisamy, M., BarathManiKanth, S., Kartikeyan, B., & Gurunathan, S. (2010). Biosynthesis of silver and gold nanoparticles using Brevibacterium casei. *Colloids and surfaces Biointerfaces*, *77*(2), 257-262.

Kalpana, V.N., payel, C., Devi, V. (2017). *Lagenaira Siceraia aided* green synthesis of ZnONps: anti-dandruff, Anti-microbail and anti-asthritic activity, *Research Journal of Chemistry and environment*, 21(11), 14-19

Kanaparthy, R., & Kanaparthy, A. (2011). The changing face of dentistry: nanotechnology. *International journal of nanomedicine*, *6*, 86-99.

Kani, T., Kani, M., Isozaki, A., Shintani, H., Ohashi, T., & Tokumoto, T. (1989). Effect to apatite-containing dentifrices on dental caries in school children. *Journal of Dental Health*, *39*(1), 104-109.

Kazarian, S. G., & Chan, K. L. A. (2006). Applications of ATR-FTIR spectroscopic imaging to biomedical samples. *Biochimica et Biophysica Acta Biomembranes*, *1758*(7), 858867.

Khan, R., & Fulekar, M. H. (2016). Biosynthesis of titanium dioxide nanoparticles using Bacillus amyloliquefaciens culture and enhancement of its photocatalytic activity for the degradation of a sulfonated textile dye Reactive Red 31. *Journal of Colloid and Interface Science*, 475, 184-191.

Khaydarov R. R, Khaydarov R. A, Evgratova S. E, Scheper T. and Endres C.(2008) Nanopartides Risk and Benefits Springer, *Dordrecht, The Netherlands 2008.*

Khodashenas, B., & Ghorbani, H. R. (2019). Synthesis of silver nanoparticles with different shapes. *Arabian Journal of Chemistry*, *12*(8), 1823-1838.

Kim, H. J., & Lee, J. H. (2014). Highly sensitive and selective gas sensors using p-type oxide semiconductors: Overview. *Sensors And Actuators Chemical*, 192, 607-627.

Kim, H., Choi, J. S., Kim, K. S., Yang, J. A., Joo, C. K., & Hahn, S. K. (2012). Peptide–hyaluronate conjugate micelle-like nanoparticles encapsulating genistein for the treatment of ocular neovascularization. *Acta biomaterialia*, *8*(11), 3932-3940.

Kim, J. S., Kuk, E., Yu, K. N., Kim, J. H., Park, S. J., Lee, H. J. & Cho, M. H. (2007). Antimicrobial effects of silver nanoparticles. *Nanomedicine: Nanotechnology, Biology and Medicine*, *3*(1), 95-101.

Kim, K. J., Sung, W. S., Moon, S. K., Choi, J. S., Kim, J. G., & Lee, D. G. (2008). Antifungal effect of silver nanoparticles on dermatophytes. *Journal of Microbiology and Biotechnology*, *18*(8), 1482-1484.

Kim, S., & Barry, B. A. (2001). Reaction-induced FT-IR spectroscopic studies of biological energy conversion in oxygenic photosynthesis and transport. *The Journal of Physical Chemistry*, *105*(19), 4072-4083.

Kirthi, A., Chung, I. M., Abdul Rahuman, A., Marimuthu, S., Anbarasan, K., Padmini, P., & Rajakumar, G. (2017). Green synthesis of copper nanoparticles using Eclipta prostrata leaves extract and their antioxidant and cytotoxic activities. *Experimental and therapeutic medicine*, *14*(1), 18-24.

Klueh U, Wagner V, Kelly S, Johnson A, Bryers JD.(2000) Efficacy of Silver Coated Fabric to Prevent Bacterial Colonization and Sub-Sequent Device Based Biofilm formation. *Journal Biomedial Material Reserved, 53: 621-631*.

Konrad, M. P., Doherty, A. P., & Bell, S. E. (2013). Stable and uniform SERS signals from self- assembled two dimensional interfacial arrays of optically coupled Ag nanoparticles" Analytical. Chemistry volume 85. 6783 – 6789.

Kosmala, A., Wright, R., Zhang, Q., & Kirby, P. (2011). Synthesis of silver nano particles and fabrication of aqueous Ag inks for inkjet printing. *Materials Chemistry and Physics*, *129*(3), 1075-1080.

Kou, T., Jin, C., Zhang, C., Sun, J., & Zhang, Z. (2012). Nanoporous core–shell Cu@ Cu 2 O nanocomposites with superior photocatalytic properties towards the degradation of methyl orange. *RSC advances*, *2*(33), 12636-12643.

Kumar, B., Smita, K., Cumbal, L., Debut, A., & Pathak, R. N. (2014). Sonochemical synthesis of silver nanoparticles using starch: a comparison. *Bioinorganic Chemistry and Applications*, 66, 65-77.

Kumar, S., & Barth, A. (2010). Following enzyme activity with infrared spectroscopy. *Sensors*, *10*(4), 2626-2637.

Lee, D. K., Kim, S. V., Limansubroto, A. N., Yen, A., Soundia, A., Wang, C. Y., & Ho, D. (2015). Nanodiamond–gutta percha composite biomaterials for root canal therapy. *ACS nano*, *9*(11), 11490-11501.

Leung, T. C. Y., Wong, C. K., & Xie, Y. (2010). Green synthesis of silver nanoparticles using biopolymers, carboxymethylated-curdlan and fucoidan. *Materials chemistry and physics*, *121*(3), 402-405.

Li, C., Wang, X., Chen, F., Zhang, C., Zhi, X., Wang, K., & Cui, D. (2013). The antifungal activity of graphene oxide–silver nanocomposites. *Biomaterials*, *34*(15), 3882-3890.

Li, C., Wu, C., Zheng, J., Lai, J., Zhang, C., & Zhao, Y. (2010). LSPR sensing of molecular biothiols based on noncoupled gold nanorods. *Langmuir*, *26*(11), 9130-9135.

Li, L. S., Hu, J., Yang, W., & Alivisatos, A. P. (2001). Band gap variation of size-and shapecontrolled colloidal CdSe quantum rods. *Nano letters*, *1*(7), 349-351.

Li, L., Pan, H., Tao, J., Xu, X., Mao, C., Gu, X., & Tang, R. (2008). Repair of enamel by using hydroxyapatite nanoparticles as the building blocks. *Journal of Materials Chemistry*, *18*(34), 4079-4084.

Li, W. R., Xie, X. B., Shi, Q. S., Zeng, H. Y., You-Sheng, O. Y., & Chen, Y. B. (2010). Antibacterial activity and mechanism of silver nanoparticles on *Escherichia coli*. *Applied microbiology and biotechnology*, *85*(4), 1115-1122.

Lim, J., Tilton, R. D., Eggeman, A., & Majetich, S. A. (2007). Design and synthesis of plasmonic magnetic nanoparticles. *Journal of Magnetism and Magnetic*, 66, 34-49.

Lin, J., Huang, Z., Wu, H., Zhou, W., Jin, P., Wei, P. & Wen, L. (2014). Inhibition of autophagy enhances the anticancer activity of silver nanoparticles. *Autophagy*, *10*(11), 2006-2020.

Liu, H. L., Dai, S. A., Fu, K. Y., & Hsu, S. H. (2010). Antibacterial properties of silver nanoparticles in three different sizes and their nanocomposites with a new waterborne polyurethane. *International Journal of Nanomedicine*, *5*, 56-66.

Liu, H., & Webster, T. J. (2007). Nanomedicine for implants: a review of studies and necessary experimental tools. *Biomaterials*, *28*(2), 354-369.

Liu, J., Wang, Z., Liu, F. D., Kane, A. B., & Hurt, R. H. (2012). Chemical transformations of nanosilver in biological environments. *ACS nano*, *6*(11), 9887-9899.

Liu, P., Huang, Z., Chen, Z., Xu, R., Wu, H., Zang, F., and Nanotechonolgy Gu, N. (2013). Silver nanoparticles: a novel radiation sensitizer for glioma. *Nanoscale*, *5*(23), 11829-11836.

Liu, Q., Douglas, T., Zamponi, C., Becker, S. T., Sherry, E., Sivananthan, S., & Warnke, P. H. (2011). Comparison of in vitro biocompatibility of NanoBone® and BioOss for human osteoblasts. *Clinical Oral Implants Research*, *22*(11), 1259-1264.

Lombardo, M., Ikuno, A. A, Baldassi L; Ferreira V. C. A (2004); Kiyota S; Evalution of Proteins Fractions from *Senna Occidentalis* Seeds extract for Cytotoxic, Antiviral and Antibacterial activities. *Virus reviews and research, 9(2), 61- 68.*

Lu, H., Lee, Y., Oguri, M., Powers, J. (2006). Properties of a dental resin composite with a spherical inorganic filler. Operat. Dentistry 31 (6), 734.

Luo, J. J., Masson, S., Behera, S., Shingu, S., & Yamagata, T. (2005). Seasonal climate predictability in a coupled OAGCM using a different approach for ensemble forecasts. *Journal of climate*, *18*(21), 4474-4497.

Mabena, L. F., Ray, S. S., Mhlanga, S. D., & Coville, N. J. (2011). Nitrogen-doped carbon nanotubes as a metal catalyst support. *Applied Nanoscience*, *1*(2), 67-77.

Macaluso, R. T. (2009). Introduction to powder diffraction and its application to nanoscale and heterogeneous materials. *Nanoscience,* 54(6), 43-58.

Macnaghten, P., Kearnes, M. B., & Wynne, B. (2005). Nanotechnology, governance, and public deliberation: what role for the social sciences. *Science communication*, *27*(2), 268-291.

Mafuné, F., Kohno, J.Y., Takeda, Y., Kondow, T., & Sawabe, H. (2000). Formation and size control of silver nanoparticles by laser ablation in aqueous solution. *Journal of Physical and Chemical Biology,* 104, 9111–9117.

Magnusson, M. H., Deppert, K., Malm, J. O., Bovin, J. O., & Samuelson, L. (1999). Sizeselected gold nanoparticles by aerosol technology. *Nanostructured Materials*, *12*(1-4), 45-48.

Malik, M. A., O'Brien, P., & Revaprasadu, N. (2002). A simple route to the synthesis of core/shell nanoparticles of chalcogenides. *Chemistry of Materials*, *14*(5), 2004-2010.

Mansha, M., Khan, I., Ullah, N., & Qurashi, A. (2017). Synthesis, characterization and visiblelight-driven photoelectrochemical hydrogen evolution reaction of carbazole-containing conjugated polymers. *International Journal of Hydrogen Energy*, *42*(16), 10952-10961.

Marco, C., Sugata, B., Valentina, C., & Marco, L. (2020). Doped Zinc Oxide Nanoparticles: Synthesis, Characterization and Potential Use in Nanomedicine, *Applied Science* 5194(10), 54-68.

Martinez, Gutierrez F., Olive P.L, Banuelos A.(2010) "Synthesis, Characterization, and Evalution of Antimicrobial and Cytotoxic Effect of Silver and Titanium Nanoparticles". Nanomedicine: *Nanotechnology, Biology and Medicine, 6(5), 681-688.*

Masciangioli, T., & Zhang, W. X. (2003). Peer reviewed: environmental technologies at the nanoscale. *Journal of Enviromental Science,* 64(3), 34-44.

Mashrai, A., Khanam, H., & Aljawfi, R. N. (2017). Biological synthesis of ZnO nanoparticles using C. albicans and studying their catalytic performance in the synthesis of steroidal pyrazolines. *Arabian Journal of Chemistry, 10,* S1530-S1536.

Mett. J. Myers, E.Roukes, M., (2011). Comparative advantages of mechanical U10 sensors. *National Nanotechnology,* 6, 203 - 215.

Mishra, S., Singh, B. R., Singh, A., Keswani, C., Naqvi, A. H., & Singh, H. B. (2014). Biofabricated silver nanoparticles act as a strong fungicide against Bipolaris sorokiniana causing spot blotch disease in wheat. *PLoS One, 9*(5), 97-081.

Mishra, Y. K., Chakravadhanula, V. S. K., Hrkac, V., Jebril, S., Agarwal, D. C., Mohapatra, S., & Adelung, R. (2012). Crystal growth behaviour in Au-ZnO nanocomposite under different annealing environments and photoswitchability. *Journal of Applied Physics, 112*(6), 308-319.

Misra, R. D. K., Girase, B., Depan, D., & Shah, J. S. (2012). Hybrid nanoscale architecture for enhancement of antimicrobial activity: immobilization of silver nanoparticles on thiol-functionalized polymer crystallized on carbon nanotubes. *Advanced Engineering Materials, 14*(4), 93-100.

Mitra, S. B., Wu, D., & Holmes, B. N. (2003). An application of nanotechnology in advanced dental materials. *The Journal of the American Dental Association*, *134*(10), 1382-1390.

Mnyusiwalla, A., Daar, A. S., & Singer, P. A. (2003). 'Mind the gap': Science and ethics in nanotechnology. *Nanotechnology*, 14(3), 9.

Monika, G., Rajesh, S. T. & Shuchi, K. (2018) Effective Antimicrobial Activity of Green ZnO Nano Particles of *Catharanthus roseus*, *Frontiers in Microbiology*, 9(10), 33-89.

Morales- Flores N, Pal U, Sanchez Mora E, (2011). Photocatalytic behaviour of ZnO and pt incorporated ZnO Nanoparticles in Phenol Degradation. Application Catalysis A. *Advanced General Study 394(5) 269- 275.*

Muhammad, B., Tahir, R., Hafiz, M., Nasir, I., Hongbo, H. & Xuehong, Z. (2017). Silver Nanoparticles: Biosynthesis and Antimicrobial Potentialities. *International Journal of Pharmacology,* 13, 832-845.

Murphy, C. J., Sau, T. K., Gole, A. M., Orendorff, C. J., Gao, J., Gou, L., & Li, T. (2005). Anisotropic metal nanoparticles: synthesis, assembly, and optical applications. *The Journal of Physical Chemistry*, *109*(29), 13857-13870.

Nassar, M. A., Ramadan, H. R., & Ibrahim, H. M. (2011). Morphological characteristics of vegetative and reproductive growth of Senna occidentalis (L.) Link. 6(43), 66-71.

National Committee for Clinical Laboratory Standard, NCCLS, (2003). Methods for the antimicrobial susceptibility testing, *Manual of Clinical Microbiology, American Society for Microbiology,* Washington, DC. 5th Edition, 1105-1125.

Natsuki, T., Tantrakarn, K., & Endo, M. (2015). Prediction of elastic properties for single-walled carbon nanotubes. *Carbon*, *42*(1), 39-45.

Ochei, J. and Kolhatkar, A. (2000). Medical Laboratory Science, Theory and Practical. *Bacteriology antimicrobial susceptibility test.* Tata McGram-Hill Publishing company limited, New Delhi, 88, 801-804.

Ogunkunle A. T., J; Ladejobi, T. A (2006). Ethnobolanical and Phylochemical studies on some species of Senna in Nigeria. *Africa Journel of Biotechnology 5(21), 2020-2023.*

Oloninefa, S. D, Abalaka, M. E, Daniyan, S. Y & Mann, A. (2018). Phytochemical screening and antibacterial susceptibilty of whole plant of *Euphorbia heterophylla* crude extracts against selected bacteria pathogens. *Bayero Journal of Pure and Applied Science,* 11(1), 211-220.

Oloyede, F.A; Alafe, B.O and Oloyede F.M (2008). Nutrient Evaluation of nepbrolepsis bisserata (Nephrotalized Lepidiaccae, pteridophyta), Botranical lithucanica 14(4), 207-210.

Organisation WH.(2014). In World Health Organisation (Education), Antimicrobial resistance: global report on surveillance.

Pal, S., Yoon, E. J., Tak, Y. K., Choi, E. C., & Song, J. M. (2009). Synthesis of highly antibacterial nanocrystalline trivalent silver polydiguanide. *Journal of the American Chemical Society*, *131*(44), 16147-16155.

Patil, P., Rathore, V. P., Hotkar, C., Savgave, S. S., Raghavendra, K., & Ingale, P. (2016). A comparison of apical sealing ability between GuttaFlow and AH plus: An in vitro study. *Journal of International Society of Preventive & Community Dentistry*, *6*(4), 377.

Paul A.K; seifulla, R.D; west, B.J (2008). *Morinda citrifolia* L (noni) improves athlete endurance: its mechanisms of action. *Journal on Medicinal plant reserve,* 2, 154-158.

Pavithra, N., Lingaraju, K., Raghu, G., & Nagaraju, G. (2017). *Citrus maxima* (pomelo) Juice mediated eco-friendly synthesis of ZnO nanoparticles: Application to photocatalytic, electrochemical sensor and antibacterial activities spectrochimney, *Journal of Microbiology,* 185, 11 - 19.

Prasad, T.N., Kambala, V.S.R., & Naidu, R. (2013). Phyconanotechnology: Synthesis of silver nanoparticles using brown marine algae cystophora moniformis and their characterization. *Journal Application of Phycology,* 25, 177 - 182.

Radziuk, D., Skirtach, A., Sukhorukov, G., Shehukin, D., & Mohwald, H. (2007). Stabilization of silver nanoparticles by polyelectrolyts and Polycethylene glycol, macromolecules Rapid community. *Polymers,* 28, 848-855.

Raj, S., Chand Mali, S., & Trivedi, R. (2018). Green synthesis and characterization of silver nanoparticles using Enicostemma axillare (Lam.) leaf extract. *Biochemical and Biophysical Research Communications,* 98, 43-55. doi:10.1016/j.bbrc.2018.08.045

Rajeev, P., Kodikara, J., Chiu, W. K., & Kuen, T. (2013). Distributed optical fibre sensors and their applications in pipeline monitoring. *Engineering Materials*. 558, 424-434.

Ram. P. & Vyshnava, S. S. (2013). Antibacterial Activity of Silver Nanoparticles Synthesized by Bark Extract of *Syzygium cumini*, *Journal of Nanoparticles*, 43(12), 6-18.

Ramsay, S. (2001). Ethical implications of research on the human genome. *The Lancet*, *357*(9255), 535.

Rasheed, T., Bilal, M., Iqbal, H. M. N., & Li, C. (2017). Green biosynthesis of silver nanoparticles using leaves extract of Artemisia vulgaris and their potential biomedical applications. *Colloids and Surfaces Biointerfaces*, 158, 408–415.

Raval, C., Vyas, K., Gandhi, U., Patel, B., & Patel, P. (2016). Nanotechnology in dentistry: A review. *Journal of Advanced Medical and Dental Sciences Research*, *4*(3), 51.

Ripp, S., & Henry, T. B. (2011). *Biotechnology and nanotechnology risk assessment: minding and managing the potential threats around us*. *American Chemical Society,* 1079, 77.

Robinson, C., Connell, S., Kirkham, J., Shore, R., & Smith, A. (2004). Dental enamel-a biological ceramic: regular substructures in enamel hydroxyapatite crystals revealed by atomic force microscopy. *Journal of Materials Chemistry*, *14*(14), 2242-2248.

Roy, L., Holm, .G, Doll, J., Holm, E., Pancho, J., & Herberger, J. (2004). World weeds: Natural Histories and Distribution of *Cassia Occidentalis* and *cassia tora* L. New York: John WIley & Sons; 1129.

Rudra, A., Banerjee, S. Singhai, N. Barua, M. Mukerji, S., and chakra- bart, B (2014). Translation and usability of autism screening and diagnostic tools for autism spectrum conditions in india. *Translation Autism research,* 7, 598-607.

Sadat-Shojai, M., Atai, M., Nodehi, A., & Khanlar, L. N. (2010). Hydroxyapatite nanorods as novel fillers for improving the properties of dental adhesives: Synthesis and application. *Nature,* 65, 55.

Sadat-Shojai, M., Atai, M., Nodehi, A., & Khanlar, L. N. (2010). Hydroxyapatite nanorods as novel fillers for improving the properties of dental adhesives: Synthesis and application. *Dental Materials*, *26*(5), 471-482.

Sagadevan, S., & Periasamy, M. (2014). Recent trends in nanobiosensors and their applications-a review. *Reserved Advanced Material Science*, *36*, 62-69.

Santra, S., Zhang, P., Wang, K., Tapec, R., & Tan, W. (2001). Conjugation of biomolecules with luminophore-doped silica nanoparticles for photostable biomarkers. *Analytical Chemistry*, *73*(20), 4988-4993.

Seery, M. K., George, R., Floris, P., & Pillai, S. C. (2007). Silver doped titanium dioxide nanomaterials for enhanced visible light photocatalysis. *Journal of Photochemistry and Photobiology Analytical Chemistry*, *189*(2-3), 258-263

Seil, J. T., & T.J. (2012). Webster, Antimicrobial applications of nanotechnology: methods and literature. *International Journal of Nanomedicine*, 7, 2767-2781.

Selvam, V. E. (2007). Trees and shrubs of the Maldives. *RAP Publication*, 6(12), 66-71.

Sergeev, B. M., Kasaikin, V. A., Litmanovich, E. A., Sergeev, G. B., & Prusov, A. N. (1999). Cryochemical synthesis and properties of silver nanoparticle dispersions stabilised by poly (2-dimethylaminoethyl methacrylate). *Mendeleev communications*, *9*(4), 130-132.

Shaalan, M., Saleh M., El-Mahdy, M., & El-Matbouli. M., (2016). Recent Progress in application of nanoparticles in fish medicine a review - Nanomedicine and Nanotechnology of Biomedicine 12. 701 - 710

Shaalan, M., Saleh, M., El-Mahdy, M., & El-Matbouli, M. (2016). Recent progress in applications of nanoparticles in fish medicine: a review. *Nanomedicine: Nanotechnology, Biology and Medicine*, *12*(3), 701-710.

Shamsuzzaman A., Mashrai H., Khanam R., Aljawfi R. (2015). Biological Synthesis of ZnO nanoparticles using C. albicans and studying their catalytic performance in the Synthesis of Steroidal Pyrazolines, *Arabic Journal of Chemistry*, 10, 10-16.

Shamsuzzaman, S. M. & Islam, T. A. B., (2015). Prevalence and antimicrobial susceptibility pattern of methicillin-resistant, vancomycin-resistant, and Panton-Valentine leukocidin positive Staphylococcus aureus in a tertiary care hospital Dhaka, Bangladesh. *Tzu Chi Medical Journal*, *27*(1), 10-14.

Shang, L., Wang, Y., Jiang, J., & Dong, S. (2007). pH-dependent protein conformational changes in albumin: gold nanoparticle bioconjugates: a spectroscopic study. *Langmuir*, *23*(5), 2714-2721.

Shankar, S., & Rhim, J. W. (2015). Amino acid mediated synthesis of silver nanoparticles and preparation of antimicrobial agar/silver nanoparticles composite films. *Carbohydrate polymers*, *130*, 353-363.

Sharma, V. K., Yngard, R. A., & Lin, Y. (2009). Silver nanoparticles: green synthesis and their antimicrobial activities. *Advances in colloid and interface science*, *145*(1-2), 83-96.

Shin, W. K., Cho, J., Kannan, A. G., Lee, Y. S., & Kim, D. W. (2016). Cross-linked composite gel polymer electrolyte using mesoporous methacrylate-functionalized SiO_2 nanoparticles for lithium-ion polymer batteries. *Scientific reports*, *6*(1), 1-10.

Sigmund, W., Yuh, J., Park, H., Maneeratana, V., Pyrgiotakis, G., Daga, A., ... & Nino, J. C. (2006). Processing and structure relationships in electrospinning of ceramic fiber systems. *Journal of the American Ceramic Society*, *89*(2), 395-407.

Singh, D. K., Pandey, D. K., Yadav, R. R., & Singh, D. (2013). A study of ZnO nanoparticles and ZnO-EG nanofluid. *Journal of Experimental Nanoscience*, *8*(5), 731-741.

Singleton, V.L., R., orthofer and R.M. Lamuela-Raventos, (1999). Analysis of total phenols and other oxidation substrates and antioxidants by means of folin-ciocalteu ceagent method enzymology., 299, 152-178.

Sirelkhatim, A., Mahmud, S., Seeni, A., Kaus, N. H. M., Ann, L. C., Bakhori, S. K. M., ... & Mohamad, D. (2015). Review on zinc oxide nanoparticles: antibacterial activity and toxicity mechanism. *Nano-Micro Letters*, *7*(3), 219-242.

Sivakumar, R., Jebanesan, A., Govin-darajan, M., & Rajasekar, P. (2011). Lavicidal and repellent activity of tetradecanoic acid against *Aedes aegypti* (Linn) and *culex quinque-fasciatus* (say) (Diptera; Culicidae). *Tsian Pacific Journal Tropical Medicine*, 4(1), 706-710.

Sondi, I., & Salopek-Sondi, B. (2004). Silver nanoparticles as antimicrobial agent: a case study on E. coli as a model for Gram-negative bacteria. *Journal of Colloid and Interface Science*, *275*(1), 177-182.

Song, J., Kim, H., Jang, Y., & Jang, J. (2013). Enhanced antibacterial activity of silver/polyrhodanine-composite-decorated silica nanoparticles. *ACS Applied Materials & Interfaces*, *5*(22), 11563-11568.

Stankic, S., Suman, S., Haque, F., & Vidic, J. (2016). Pure and multi metal oxide nanoparticles: synthesis, antibacterial and cytotoxic properties. *Journal of Nanobiotechnology*, *14*(1), 1-20.

Stevens, W. D., Ulloa, C., Pool, A., & Montiel, O. M. (2001). *Flora de Nicaragua* (Vol. 85, No. 1, p. 943). St. Louis: Missouri Botanical Garden Press. Pp 56-66.

Su, M., Li, S., & Dravid, V. P. (2003). Microcantilever resonance-based DNA detection with nanoparticle probes. *Applied Physics Letters*, *82*(20), 3562-3564.

Sun, L., & Chow, L. C. (2008). Preparation and properties of nano-sized calcium fluoride for dental applications. *Dental Materials*, *24*(1), 111-116.

Sun, S., Murray, C. B., Weller, D., Folks, L., & Moser, A. (2000). Monodisperse FePt nanoparticles and ferromagnetic *FePt Nanocrystal Superlattices*. *science*, *287*(5460), 1989-1992.

Suzuki, S. (2004). In vitro wear of nano-composite denture teeth. *Journal of Prosthodontics: Implant, Esthetic and Reconstructive Dentistry*, *13*(4), 238-243.

Swadeshmukul, S., Peng. Z., Kemin, W., Rovelyn. T., Weihong. T., (2001). Conguation of biomolecules with luminsophere - doped silica nanoparticles for photostable biomarkers. *Analystical Chemistry*, 73, 4988 - 4993.

Tao, A., Sinsermsuksakul, P., & Yang, P. (2006). Polyhedral silver nanocrystals with distinct scattering signatures. *Angewandte Chemical International Edition*, *45*(28), 4597-4601.

Tao, J., Pan, H., Zeng, Y., Xu, X., & Tang, R. (2007). Roles of amorphous calcium phosphate and biological additives in the assembly of hydroxyapatite nanoparticles. *The Journal of Physical Chemistry*, *111*(47), 13410-13418.

Thanh, N. T., & Green, L. A. (2010). Functionalisation of nanoparticles for biomedical applications. *Nanotechnology*, *5*(3), 213-230.

Thomas, S., Kumar Mishra, P., & Talegaonkar, S. (2015). Ceramic nanoparticles: fabrication methods and applications in drug delivery. *Current Pharmaceutical Design*, *21*(42), 61, 61-78.

Tien, D. C., Liao, C. Y., Huang, J. C., Tseng, K. H., Lung, J. K., Tsung, T. T., & Stobinski, L. (2008). Novel technique for preparing a nano-silver water suspension by the arcdischarge method. *Reserved. Advanced Material of Science*, *18*, 750-756.

Tolobic; M., Jemec, A., Drobne, D., Romih, T., Casemets, K., Kahru A., 2012. Upon exposure to

Tomsia, A. P., Launey, M. E., Lee, J. S., Mankani, M. H., Wegst, U. G., & Saiz, E. (2011). Nanotechnology approaches for better dental implants. *The International Journal of Oral and Maxillofacial Implants*, *26*, 25.

Totu, E. E., Nechifor, A. C., Nechifor, G., Aboul-Enein, H. Y., & Cristache, C. M. (2017). Poly (methyl methacrylate) with TiO2 nanoparticles inclusion for stereolitographic complete denture manufacturing– the fututre in dental care for elderly edentulous patients. *Journal of Dentistry*, *59*, 68-77.

Touhami, A. (2014). Biosensors and nanobiosensors: design and applications. *Nanomedicine*, *15*, 374-403.

Tran, Q. H., & Le, A. T. (2013). Silver nanoparticles: synthesis, properties, toxicology, applications and perspectives. *Advances in Natural Sciences: Nanoscience and Nanotechnology*, *4*(3), 033001.

Trease, E.G., & Evans, W.C. (1983). Textbook of pharmacognosy, 14th edition. W.B Sanders Company Ltd, oval Road London NWI TDX, UK. 293-334, 471-511.

Tsuji, S., Kawai, N., Tsujii, M., Kuwaro, S., & Hori, M. (2003). Infianmation related promotion of gastro-intestinal carcinogenesis a perigenetic pathway Alimentary pharmacology and therapeutics. *Journal of Biological Sciences,* 18, 82-89

Vaiano, V., Matarangolo, M., Murcia, J. J., Rojas, H., Navío, J. A., & Hidalgo, M. C. (2018). Enhanced photocatalytic removal of phenol from aqueous solutions using ZnO modified with Ag. *Applied Catalysis Biological Environmental*, 225, 197–206

Vashishtha, V. M., John, T. J., & Kumar, A. (2009). Clinical & pathological features of acute toxicity due to Cassia occidentalis in vertebrates. *Indian Journal of Medical Research*, *130*(1), 23.

Vasireddy, R., Paul, A., & Krishna Mitra, A. (2012). Green Synthesis of Silver nanoparticles and the study of optical properties". *Nanomaterials and nanotechnology*, 2, 8-19.

Vijayakumar, S., Mahadevan, S., Arulmozhi, P., Sriram, S., & Praseetha, P. K. (2018). Green synthesis of zinc oxide nanoparticles using Atalantia monophylla leaf extracts: Characterization and antimicrobial analysis. *Materials Science in Semiconductor Processing*, *82*, 39-45.

Vilchis-Nestor, A. R., Sánchez-Mendieta, V., Camacho-López, M. A., Gómez-Espinosa, R. M., Camacho-López, M. A., & Arenas-Alatorre, J. A. (2008). Solventless synthesis and optical properties of Au and Ag nanoparticles using *Camellia sinensis* extract. *Materials letters*, *62*(17-18), 3103-3105.

Wakirwa J.H., Ibrahim P., and Madu S.J., 2013, Phytochemical screening and in vitro antimicrobial analysis of the ethanol bark extract of *Jatropha curcas* Linn, *Eurphorbiaceae*. *International Research Journal of Pharmacy*, 4(3), 97-100

Wang, H. J., Yang, L., Yang, H. Y., Wang, K., Yao, W. G., Jiang, K., & Zheng, Z. (2010). Antineoplastic activities of protein-conjugated silver sulfide nano-crystals with different shapes. *Journal of inorganic biochemistry*, *104*(1), 87-91.

Wang, L., Xie, X., Li, C., Liu, H., Zhang, K., Zhou, Y., & Xu, H. H. (2017). Novel bioactive root canal sealer to inhibit endodontic multispecies biofilms with remineralizing calcium phosphate ions. *Journal of dentistry*, *60*, 25-32.

Wang, R., Xin, J. H., Yang, Y., Liu, H., Xu, L., & Hu, J. (2004). The characteristics and photocatalytic activities of silver doped ZnO nanocrystallites. *Applied Surface Science*, *227*(1-4), 312-317.

Wang, Y., & Xia, Y. (2004). Bottom-up and top-down approaches to the synthesis of monodispersed spherical colloids of low melting-point metals. *Nano letters*, *4*(10), 20472050.

Wang, Z. L. (2000). Transmission electron microscopy of shape-controlled nanocrystals and their assemblies. *Nanoscioence*, 6(5), 66-74.

Wei, L., Lu, J., Xu, H., Patel, A., Chen, Z. S., & Chen, G. (2015). Silver nanoparticles: synthesis, properties, and therapeutic applications. *Drug Discovery Today*, *20*(5), 595-601.

Weiss, J., Takhistov, P., & McClements, D. J. (2006). Functional materials in food nanotechnology. *Journal of Food Science*, *71*(9), 107-116.

Wiley, B., Sun, Y., Mayers, B., & Xia, Y. (2005). Shape-controlled synthesis of metal nanostructures: the case of silver. *Chemistry–A European Journal*, *11*(2), 454-463.

Wong, K. K., Cheung, S. O., Huang, L., Niu, J., Tao, C., Ho, C. M., & Tam, P. K. (2009). Further evidence of the anti-inflammatory effects of silver nanoparticles. *Nanoscience*, 4(3), 44-57.

World Health Organisation (WHO 2012)- The evolving threat of antimicrobial resistance-*options for action. Geneva.*

Wu, H., He, L., Gao, M., Gao, S., Liao, X., & Shi, B. (2011). One-step in situ assembly of sizecontrolled silver nanoparticles on polyphenol-grafted collagen fiber with enhanced antibacterial properties. *New Journal of Chemistry*, *35*(12), 2902-2909.

Wu, J. J., & Tseng, C. H. (2006). Photocatalytic properties of nc-Au/ZnO Nanorod Composites. *Applied Catalysis Bio-Environmental*, *66*(1-2), 51-57.

Wu, J., Zhou, H., Weir, M. D., Melo, M. A. S., Levine, E. D., & Xu, H. H. (2015). Effect of dimethylaminohexadecyl methacrylate mass fraction on fracture toughness and antibacterial properties of CaP nanocomposite. *Journal of Dentistry*, *43*(12), 1539-1546.

Wu, P., Gao, Y., Lu, Y., Zhang, H., & Cai, C. (2013). High specific detection and near-infrared photothermal therapy of lung cancer cells with high SERS active aptamer–silver–gold shell–core nanostructures. *Analystical*, *138*(21), 6501-6510.

Yao, H., & Kimura, K. (2007). Field emission scanning electron microscopy for structural characterization of 3D gold nanoparticle superlattices. *Modern Research and Educational Topics in Microscopy*, *2*, 568-576.

Yedurkar, S., Maurya, C., & Mahanwar, P. (2016). Biosynthesis of zinc oxide nanoparticles using ixora coccinea leaf extract—a green approach. *Open Journal of Synthesis Theory and Applications*, *5*(1), 1-14.

Zawrah, M. F., Zayed, H. A., Essawy, R. A., Nassar, A. H., & Taha, M. A. (2013). Preparation by mechanical alloying, characterization and sintering of Copper–20 wt.% Al_2O_3 nanocomposites. *Materials & Design*, *46*, 485-490.

Zhang, Q., Li, N., Goebl, J., Lu, Z., & Yin, Y. (2011). A systematic study of the synthesis of silver nanoplates: is citrate a magic reagent. *Journal of the American Chemical Society*, *133*(46), 18931-18939.

Zhu, J. J., Liao, X. H., Zhao, X. N., & Chen, H. Y. (2001). Preparation of silver nanorods by electrochemical methods. *Materials Letters*, *49*(2), 91-95.

APPENDIX

Plate VI: Biosynthesised Zinc Nanoparticles (Solid)

Plate VII: Biosynthesised of Silver Nanoparticle (Liquid)

Plate VIII: Antimicrobial activity of Zinc nanoparticle

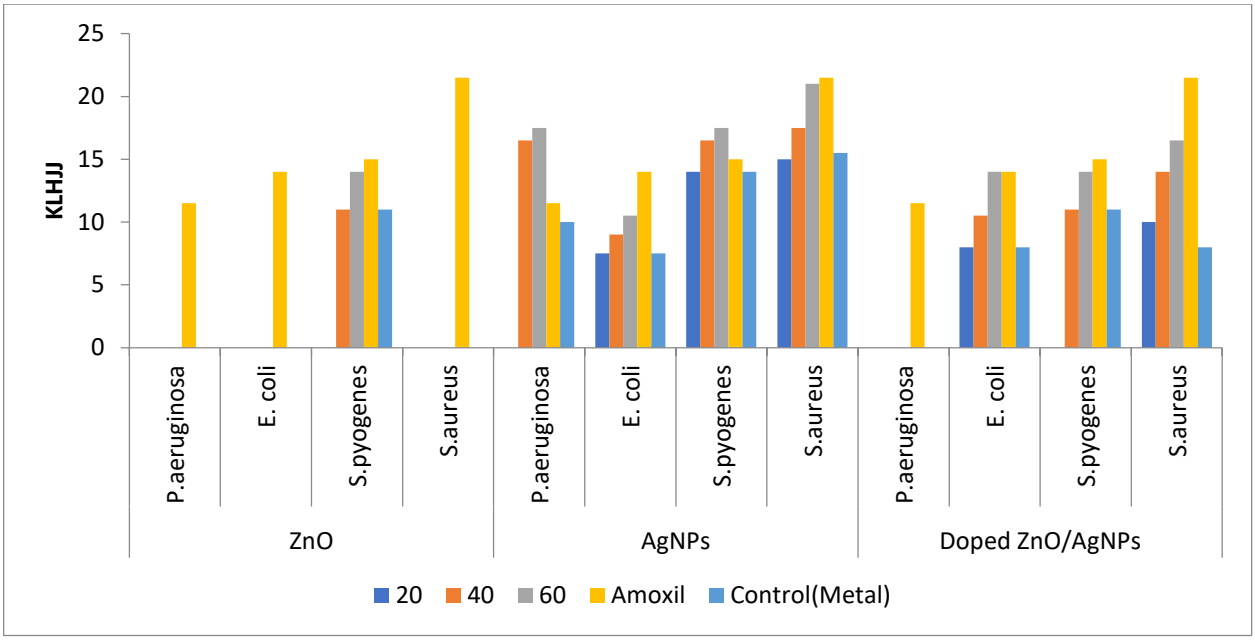

Table 4.1: Antimicrobial susceptibility test result

Plate IX: Antimicrobial activity of Silver nanoparticle

Plate X: Antimicrobial activity of Doped Zinc and Silver nanoparticle